Graphical Abstract

Non-covalent Interactions

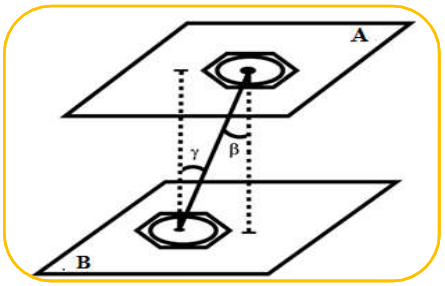

π–π stacking

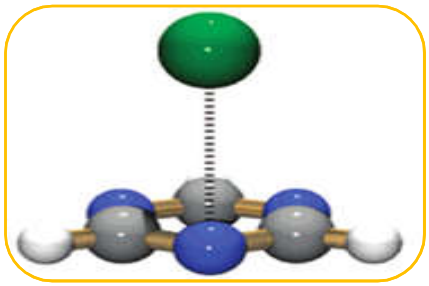

Anion-π

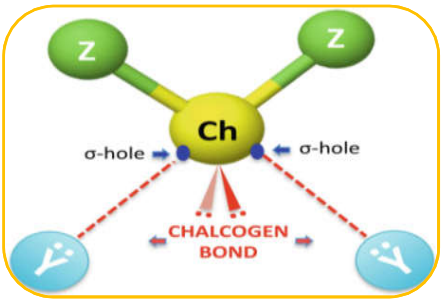

σ-hole

QTAIM

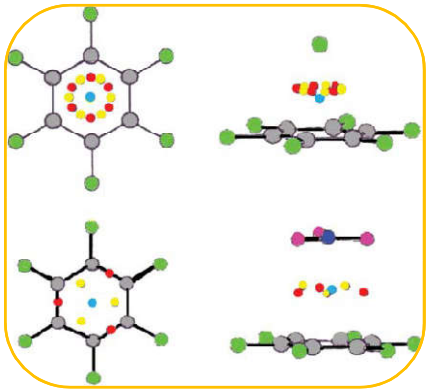

MEP

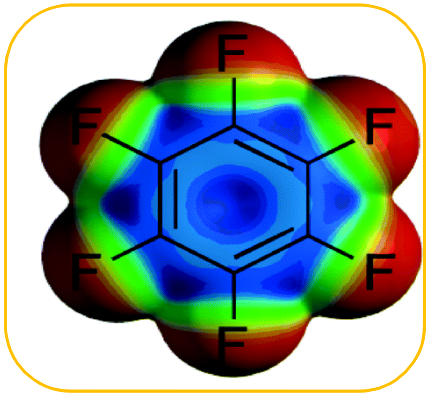

NCI

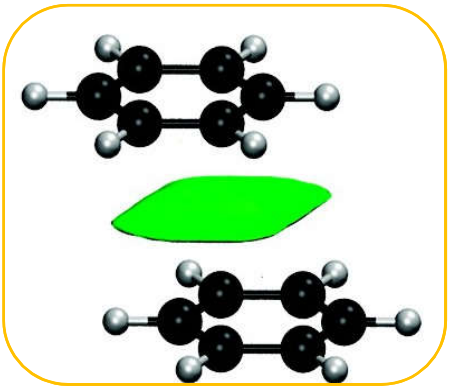

Crystal Engineering

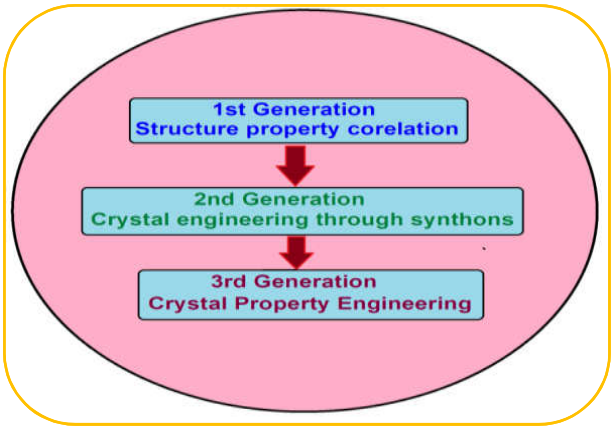

Metallosupramolecular Chemistry

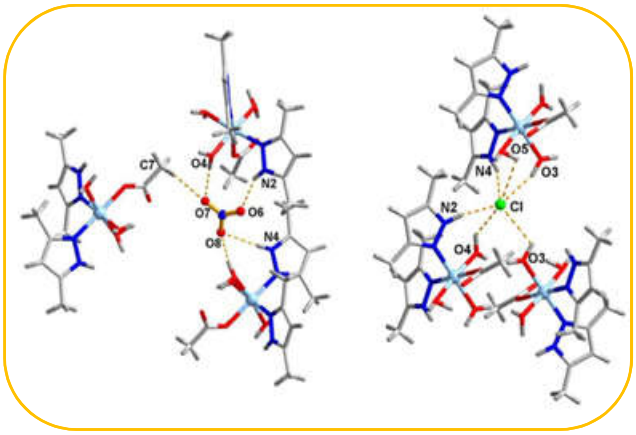

Cell Cycle

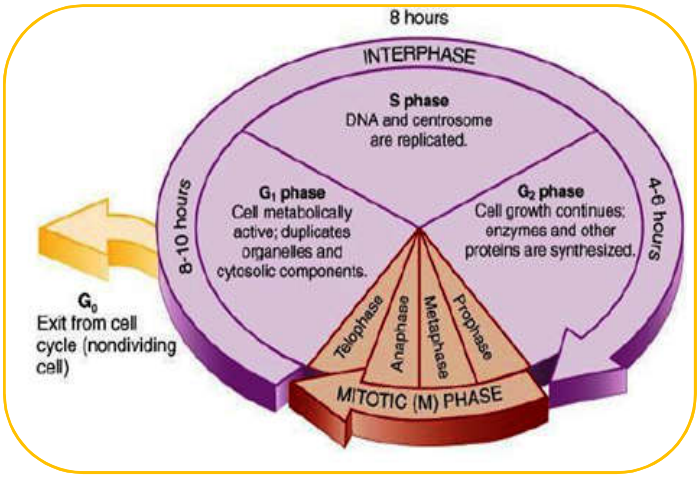

Apoptosis

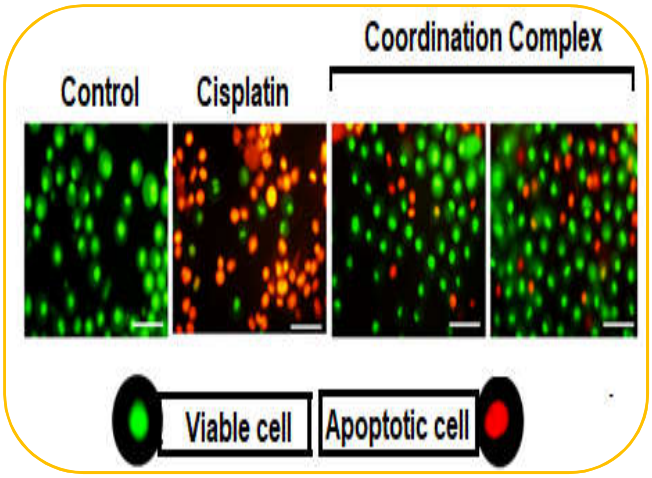

General Introduction

1. General Introduction

Nature always inspires researchers for the development of novel materials useful for mankind. As a consequence, there are ongoing attempts to design and develop invaluable materials in the form of natural products,[1] clinically approved drugs,[2] nanomaterials,[3] and electronic devices.[4] However, the synthesis of such novel, structurally-exquisite compounds/molecules is quite challenging, where every group and atom has a precise destination within a targeted framework. Owing to the depth knowledge of the reaction systems, researchers are trying to take precise control over material synthesis and their reactivity and attempting to construct complex compounds of desired dimensionalities.[5] Linus Pauling has successfully exploited the nature of covalent bonding in the 1930s,[6] but still, chemists are unable to take control on the interactions of reactant molecules. It has been explored that the biological systems are capable of influencing molecules and building more complex molecules by exerting dynamic control over non-covalent interactions with definite precision.[7] To explore and visualize the interplay of non-covalent interactions in the self assembly processes during molecular association, a new discipline named *Supramolecular Chemistry* has emerged along with the development of a wide number of sub-branches including molecular recognition, host-guest chemistry and self-assembly processes.

1.1 Supramolecular Chemistry

Supramolecular chemistry can be defined as "*the chemistry of the intermolecular bonds, covering the structures and functions of the entities formed by association of two or more chemical species*", or more colloquially as "*chemistry beyond the molecules*".[8]

Supramolecular chemistry has emerged as a fast growing research area in chemistry, covering a wide range of research fields starting from biological chemistry to material science, and from synthesis to spectroscopic studies.[9]

Supramolecular chemistry focuses on the reversible "*intermolecular bond*", aims at controlling the non-covalent intermolecular forces (**Figure 1.1**) responsible for the "*association of two or more chemical species*"[10] for the construction of interesting complex compounds with organized architectures.

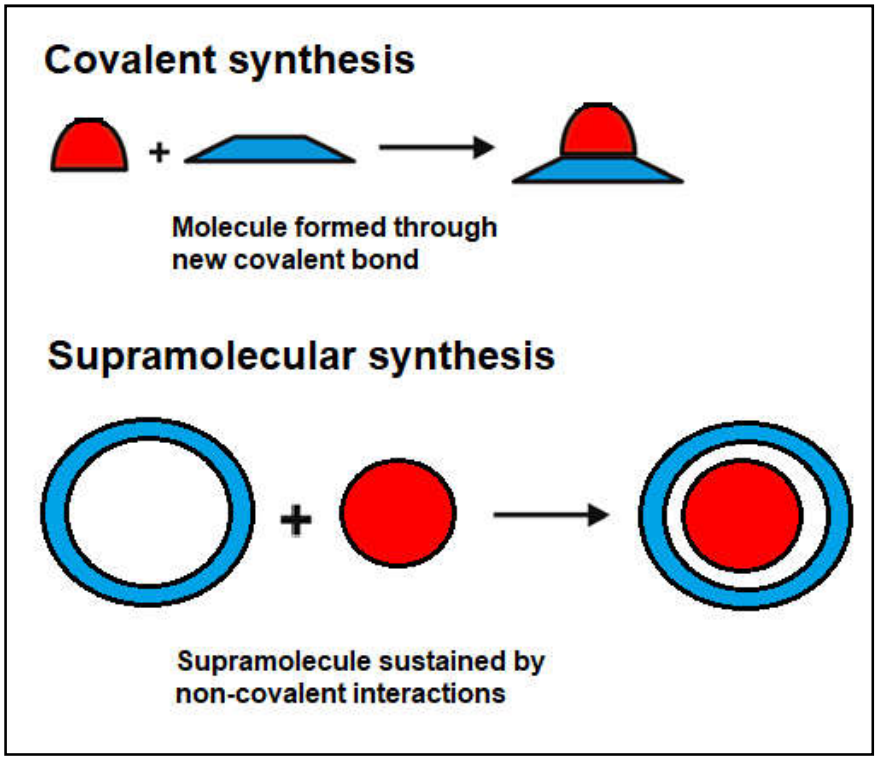

Figure 1.1 Molecular and supramolecular chemistry.

1.2 Non-covalent Interactions

The non-covalent interactions include a large number of molecular interactions that include metal-ligand (M-L) coordination, hydrogen-bonding, π-donor-π-acceptor interactions and van der Waals interactions (**Figure 1.2**). The strength and directionality of these interactions are quite different ranging from a few hundred kilojoules per mole for the strongest interactions (typically ~200 $kJmol^{-1}$ for M-L coordination bonds) to a few kilojoules per mole for the weakest ones (2-25 $kJmol^{-1}$ for hydrogen bonds or π-π interactions). The reversible character of these interactions makes it challenging and difficult to gain control over the forces responsible for the formation of the complex systems. However, because of the thermodynamic control of such interactions, supramolecular entities possess the capability of "*self correction*".[11]

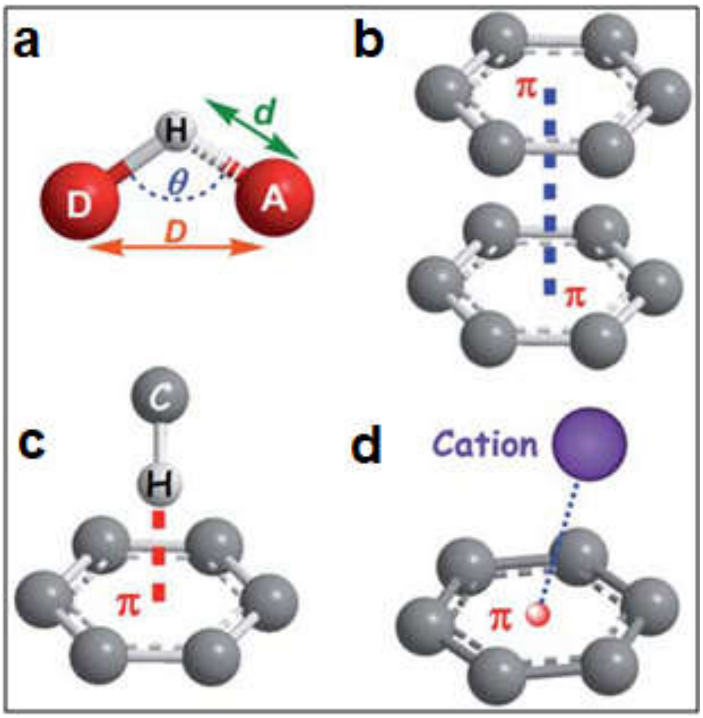

Figure 1.2(**a**) Hydrogen-bond, (**b**) π–π, (**c**) C–H···π and (**d**) cation–π interactions.

1.2.1 Hydrogen Bonding

Hydrogen bonds (H-bonds) are considered to be the most widespread elemental supramolecular forces experienced in nature.[12] They are simply the attractive interaction between the hydrogen atom attached to an electronegative atom (termed as the hydrogen bond donor, D) and an atom or a group of atoms in the same or a different molecule (termed as hydrogen bond acceptor, A).[13] Typical hydrogen bonds may be depicted as X–H···Y–Z, where the three dots denote the hydrogen bond, X is the hydrogen bond donor atom/group. The acceptor may be an atom or an anion Y, or a fragment or a molecule Y–Z, where Y is bonded to Z. Depending on the electrostatic interactions between atoms or groups of atoms from a different molecule or belonging to the same molecule, hydrogen bonds are classified as intermolecular and intramolecular hydrogen bond respectively.[14] The bond energy associated with these bonds are found to be stronger than that of other usual intermolecular interactions, however they are fairly weak compared to covalent bonds. Various factors such as the electronegativities of the donor and acceptor atoms, pressure, temperature, bond angle, bond distance and the overall chemical environment influence the strength of hydrogen bonds.[15] Hydrogen

bonds are directional and reversible interactions whose energy usually ranges from 4-40 kcalmol^{-1}.[16] The shorter hydrogen-acceptor (H-A) distance indicates the presence of stronger hydrogen bond whereas the deviation of D–H···A angle from ideal conditions (tends towards 180°) makes the interaction much weaker.[17] The weak nature of C–H···O hydrogen bonds can be corroborated by the commonly observed smaller angles that is usually as low as 120°.

Different conformations of the hydrogen bonding interactions also play crucial role in their bond strength. The most common conformations *viz*. simple, bifurcated, trifurcated, bridge, cyclic and cyclic dimer are depicted in **Figure 1.3**.

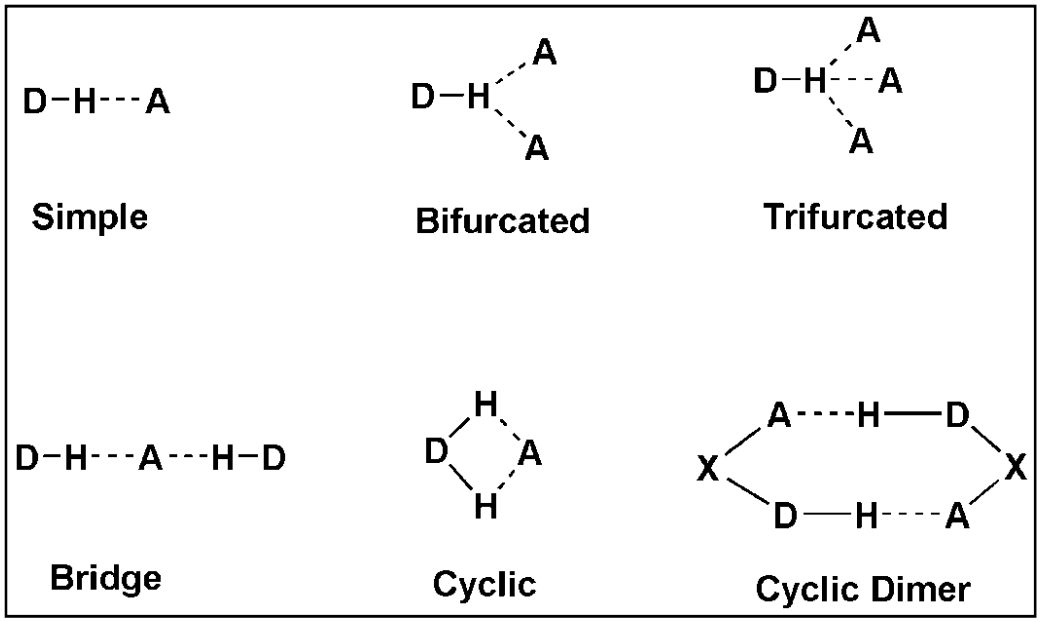

Figure 1.3 Most common conformations for hydrogen bonding interactions.

Table 1.1 Classification of hydrogen bonds according to their strength and geometric parameters.

Properties	Strong	Moderate	Weak
D–H···A interaction	Important covalent component	Mainly electrostatic	van der Waals
Bond length	D–H ~ H···A	D–H < H···A	D–H << H···A
H···A (Å)	~ 1.2-1.5	~ 1.5 - 2.0	~ 2.0 - 3.0
D···A (Å)	2.2-2.5	2.5 - 3.2	3.0 - 4.0
Bond angles (º)	175-180	130 - 180	90 - 150
Bond energy (kcalmol^{-1})	14-40	4 -15	<4
Relative IR shift (cm^{-1})	25	10 - 25	<10
^{1}H NMR Chemical shift (ppm)	14-22	<14	----

As a function of bond distances and bond angles, H-bonds can be classified as strong, moderate and weak.[18] **Table 1.1** represents the classification of H-bonds along with various parameters. Although H-bonds are the simplest and weak non-covalent interactions in molecular assemblies, such bonds can play crucial role in the stabilization of supramolecular network architectures when participate in large numbers.[19]

Detailed experimental and theoretical analysis of H-bonding interactions reveals three different kinds of H-bonds *viz*. typical conventional H-bonds (designated as D−H···A) with the positive charge on H-atom; inverse (or hydride) bonds where a negatively charged hydrogen atom is situated between electropositive atoms; and dihydrogen bonds (DHBs) D−H···H−A containing both protic and hydric H-atoms.[20] It is reported in the literature that the properties of DHBs do not differ much from typical conventional H-bonds and the formation of DHBs usually causes changes similar to those of conventional hydrogen bonds.

The non-covalent hydrogen bond has a great importance in biological systems. They play prominent role in the formation and stabilization of 3D structures of proteins and nucleic acids.[21] In biological macromolecules, the coupling between different parts of the macromolecule via non-covalent interactions originates specific structures that determine the biological and physiological roles. The formation of double helix of DNA is mainly due to the involvement of H-bonds and π-π stacking interactions between the nucleotide base-pairs. The mechanisms of action of anticancer chemotherapeutic drugs that are currently used worldwide (e.g. cisplatin, carboplatin) are based on their intercalation in the DNA through H-bonds.[21a]

1.2.2 Graph Set Definitions

Graph set approach is usually used for the simple representation of complicated H-bonded supramolecular networks by four different simple patterns, each of which is specified by a designator *viz*. chains (**C**), rings (**R**), intramolecular H-bonded patterns (**S**), and other finite patterns (**D**). In the specification of each pattern, the subscript represents the number of H-bond donors (**d**) and the superscript gives the number of H-bond acceptors (**a**). Moreover, the total number of atoms (**n**) involved in the pattern is called the degree of the pattern. The graph set descriptor is represented as $G_d^a(n)$ [where, **G** represents one of the four possible designators]. This approach was

originally developed by M. C. Etter to utilize patterns of H-bonding for the understanding and the design of molecular crystals.[22]

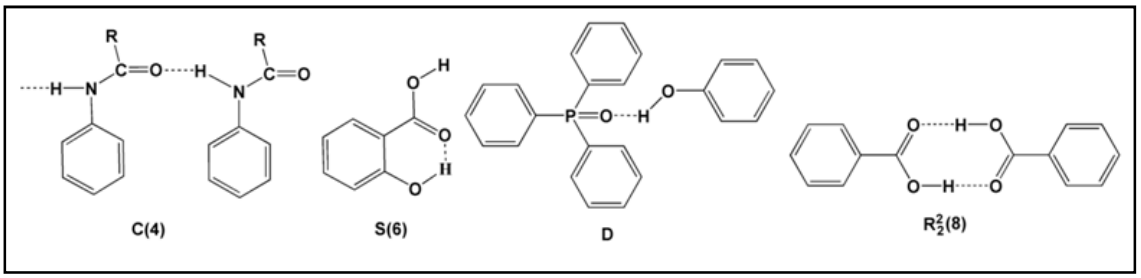

Figure 1.4 Four patterns of graph set notation.

Four different patterns of graph set notation are shown in **Figure 1.4**. A supramolecular chain composed of four atoms can be specified as **C**(**4**). Absence of subscript and superscript in a graph set notation implies one donor and one acceptor atoms. The intramolecular H-bond comprising of six atoms can be specified as **S**(**6**). The designation **D** is used when the donor and acceptor are from two (or more) discrete entities (molecules or ions) that involve only one donor and one acceptor and the pattern involves only the hydrogen bond. In such a case, other atoms need not be counted and the degree of the pattern (**n**) may be omitted. Finally, the fourth possible pattern shown contains eight atoms, two of them donors and two acceptors and hence is designated as $R_2^2(8)$.

1.2.3 π-π Interactions

π-π stacking interactions between molecular units in supramolecular architectures can be referred to the intermolecular overlapping of p-orbitals involving π-conjugated systems. In π-π stacking interactions, parameters such as aromatic ring centroid-centroid distance (3.3-4.0 Å), centroid plane distance (3.3-4.1 Å) and dihedral angle between the planes of the rings (α = 0-19º) are taken into account. To measure the displacement of one ring over the other, the angles, γ and β are used as shown in **Figure 1.5**. These angles are formed between the centroid-centroid vectors and centroid-layer for both the rings.

Computational electrostatic models have been proposed to explain this phenomenon, whereby the π-system of an electron rich aromatic molecule attracts the

electron deficient π-system of another aromatic molecule so that the expected usual π-π electronic repulsion that destabilizes the complex is disfavoured.[23] These types of non-covalent interactions are quite important in biological systems as illustrated by the stabilization of the double helical structure of DNA through vertical π-stacked base-base interactions and the tertiary structure of proteins.[24]

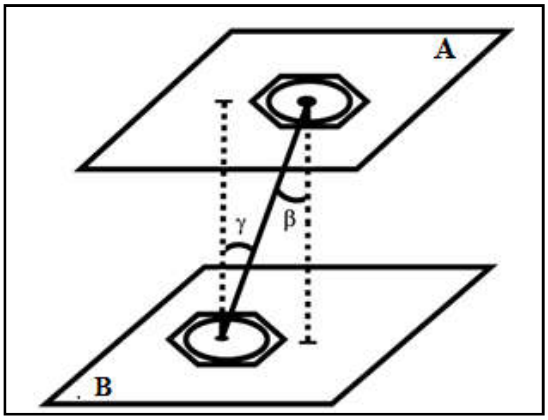

Figure 1.5 Parameters for π–π stacking interactions.

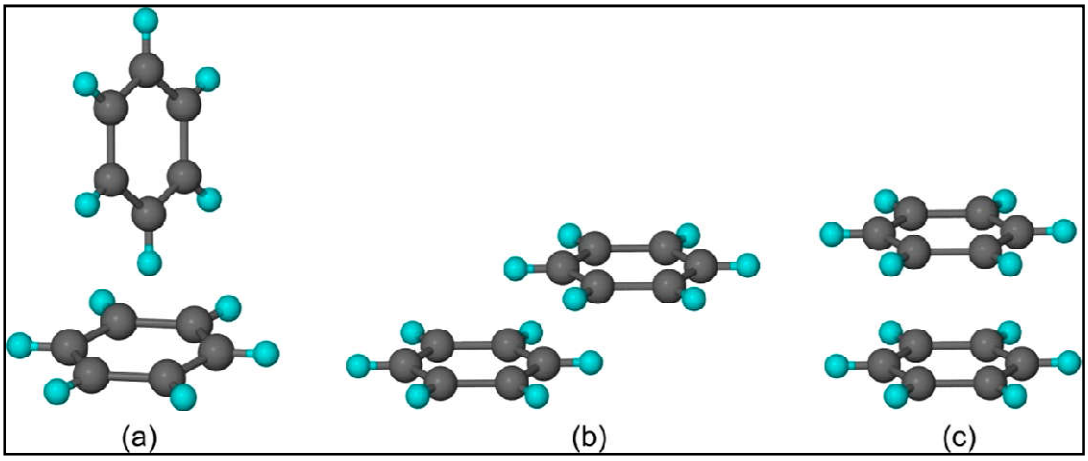

Figure 1.6(a) Edge-to-face T-shaped, (**b**) parallel displaced and (**c**) cofacial parallel stacked geometries of π-π stacking interactions between aromatic systems.

On the basis of geometry, the π-π interactions between two aromatic species can be broadly classified into three categories: edge-to-face T-shaped, parallel displaced, and cofacial parallel stacked (**Figure 1.6**).[25] The small, unsubstituted aromatic compounds prefer edge-to-face T-shaped geometry, whereas substituted and large

multi-ring aromatic compounds prefer parallel displaced geometry. Cofacial parallel stacked geometry is rather rarely observed.

Sanders and Hunters have explained π-π interactions in terms of a quadrupole moment with partial negative electrostatic potential above both the aromatic faces and a partial positive electrostatic potential around the periphery for the benzene type of molecules.[26] They have shown that two such quadrupole moments in proximity should prefer edge-to-face T-shaped or parallel displaced stacking geometry over cofacial parallel stacked geometry. If strong electron withdrawing groups are attached to the aromatic ring (hexafluorobenzene), a reverse of polarization can be observed, which leads to a quadrupole moment with partial positive electrostatic potential above both the aromatic faces and a partial negative electrostatic potential around the periphery. Sherrill and co-workers have theoretically predicted that among the three geometries, T-shaped and parallel displaced are the most stable and nearly isoenergetic, whereas the cofacial parallel stacked geometry is least favoured in the case of benzene dimers.[27]

1.2.4 Applications of π-π Interactions

After the enormous role of π-π interactions in supramolecular chemistry has been realized, it has gained immense interest in research areas ranging from material science to molecular biology. π-π stacking interactions are known to play a vital role in the thermal stability and folding of proteins. Iverson and co-workers have exploited complementary π-π stacking in folding of pyridine-pyridazine oligomers into a pleated structure even in water.[28] Devices with excellent photoconductivity have been achieved in the π-stacked single component as well as multi-component organic crystals.[29] π-π stacking interaction has been found to play a vital role in forming efficient charge transport channels for both small molecules as well as polymeric semiconducting materials.[30] Stoddart and co-workers employed π-electron-rich and π-electron-deficient species to design molecular shuttle (*molecular assembly in which macrocyclic ring is able to move back and forth between two recognition sites*) which can be induced by chemical and electrochemical processes.[31] π-π interaction has also been employed in sensing nitro aromatic based explosives.[32]

As most of the clinically approved chemical drugs possess aromatic rings, π-π stacking interactions have a major role in the design of chemical drug-delivery systems. In the process of developing chemical drugs, the balance between hydrophilicity and

lipophilicity is considered to be important for absorption and distribution of drug throughout the body.[33] For most of the drugs, lipophilicity is conferred by the presence of aromatic ring structures. The presence of aromatic rings that show self-assembly via π-stacking interactions in drugs facilitates the loading of such drugs into delivery systems.

This π-π stacking interaction plays an important role in the stabilization of DNA; together with hydrogen bond, such stacking results in pair-base stacking that generates characteristic helicoidal structure. Based on this, a number of intercalating drugs have been designed. On the other hand, π-π stacking interactions have a lot of applications in supramolecular host-guest systems.[34]

1.2.5 Cooperative Non-covalent Interactions

Cooperativity of non-covalent interactions is one of the key concepts for understanding molecular association and self-assembly processes in metal-organic chemistry.[35] There are many evidences of cooperative interplay of non-covalent interactions in supramolecular assemblies, yet there is an universal perplexity regarding the definition and quantification of this phenomena, particularly in the context of self-assembled architectures.[36] Cooperativity arises from the interplay of two or more non-covalent interactions in supramolecular architectures, so that the whole system behaves differently from the expectations based on the properties of the individual interactions in isolation. Interplay of non-covalent interactions can lead to either positive or negative cooperativity, depending on whether one interaction favours or disfavours another. Cooperativity is one of the most important properties of the molecular systems observed in biological fields (**Figure 1.7**).[37] Cooperative aggregations in micelle formation and intermolecular cooperativity in host-guest assemblies are involved in the formation of larger aggregates or discrete metal-organic complexes. Cooperative interplay of non-covalent interactions has widespread importance in nature as they play crucial roles in the configuration of 3D protein structures.[38]

The cooperative action of π-stacking interactions is also observed in supramolecular assemblies of coordination solids.[39] The dispersive π-stacked interactions play an increasingly crucial role in the stability of proteins or nucleic acids and in the recognition of drugs by enzymes.[40] A molecular entity of π-system comprising many electron rich and electron deficient rings; understanding of how two

π^+/π^- rings would interact each other and be assembled in the crystal structure is a very intriguing subject for the study of π–π cooperative stacking interactions.[41] Theoretical calculations on crystal structures have established the cooperative interplay of π-stacked assemblies with hydrogen bonding, halogen bonding and metal coordination; the calculations revealed that the electrostatic enhancement of such interactions are due to remarkable cooperativity effects.[42]

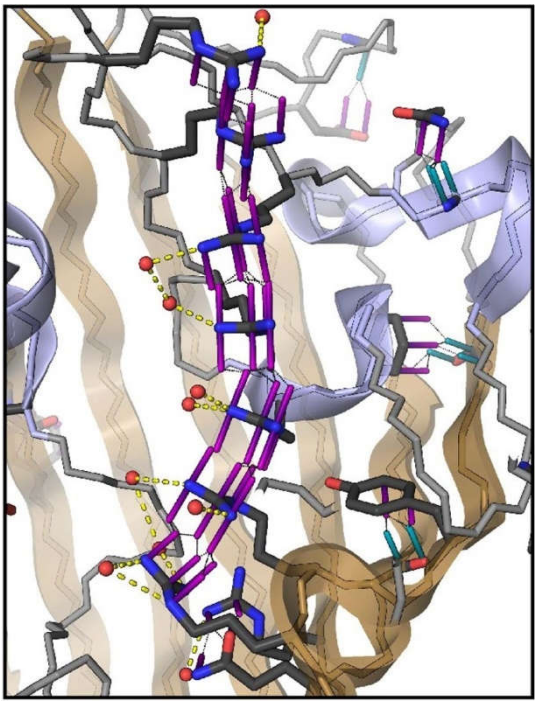

Figure 1.7 Cooperative π-π contacts in folded protein structures.[43]

1.2.6 CN···CN Interactions

In 1968, H. A. Bent highlighted the importance of non-covalent interactions between strongly dipolar groups.[44] In recent times, the interaction between dipolar carbonyl groups has gained emphasis due to their prominent role in stabilizing various supramolecular network architectures.[45] However, several other chemical groups exhibit local dipole moments similar to that of the carbonyl groups and thereby providing stability to the crystal structures. Among these, nitrile groups are of particular interest from the viewpoint of crystal engineering (*vide infra*) because of their key role in determining molecular packing via CN···CN interactions. As a polar functional group, the nitrile moiety engages in dipole-dipole interactions, which help to stabilize the

network architectures.[46] The nitrile group is reported to serve as an H-bond acceptor in coordination complexes, frequently participating in relatively weak and unconventional H-bonding and also takes part in commonly occurring H-bonding interactions.[47] This group is also reported to play the role of a Lewis base in the network architectures of crystalline solids that is capable of interacting with Lewis acids, particularly with halogen atoms of neighbouring molecules.[48]

The Cambridge Structural Database (CSD)[49] analysis shows that CN···CN interactions is formed in an analogous manner to those involving carbonyl groups, and with the similar interaction motifs *viz*. (i) anti-parallel motif, (ii) sheared parallel motif and (iii) perpendicular motif among which anti-parallel motif is the dominant one.[50]

1.2.7 σ-hole Interactions

A σ-hole can be described as the region of positive electrostatic potential found on an (partially) empty anti-bonding σ* orbital, located along a covalent bond. The concept of σ-hole was originally used to explain the unconventional interaction of an electronegative halogen atom (Hl) with a negative site, wherein the electropositive potential is found on the halogen atom at the end of the X-Hl σ-bond (X can be any atom, but is commonly carbon).[51] It was then reported that such electronic anisotropy is not unique to atoms of the halogen family and σ-holes are also found on covalently bonded atoms of the tetrel (group 14), pnictogen (group 15) and chalcogen (group 16) families.[52,53]

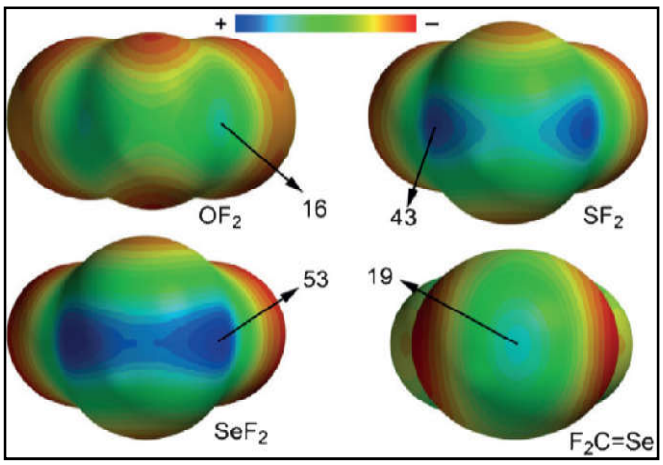

Figure 1.8 Molecular electrostatic potential (kcal/mol) of representative σ-hole chalogen bonding interactions.[54]

σ-hole interactions can be represented as X-D···A (where X can be any atom, D = donor atom and A = acceptor moiety) which is quite similar to hydrogen bonding.[55] When the donor atom is more polarizable (heavier atoms) or X is more electron withdrawing, then σ-hole becomes more positive.[56] Although σ-hole bonding interaction is greatly influenced by electrostatic interactions, other forces such as polarization and dispersion also play important roles.[57] Increase in the polarizability also increases the magnitude of the σ-holes and strengthens the resulting σ-hole complexes.

It is well known that the polarizabilities of the atoms in the second row of the periodic table are very modest and they increase significantly upon going from row 2 to 5. To illustrate this trend, the molecular electrostatic potential (MEP) surface plots (*vide infra*) of several YF_2 molecules (Y = O, S and Se) and F_2C=Se are shown in **Figure 1.8**. Two σ-holes are present for the YF_2 molecules on the extensions of each covalent Y-F bond. The MEP value (53 kcal/mol) at the σ-hole of the SeF_2 molecule is largest; corroborating the most polarizable nature of Se (five times more than O).[54]

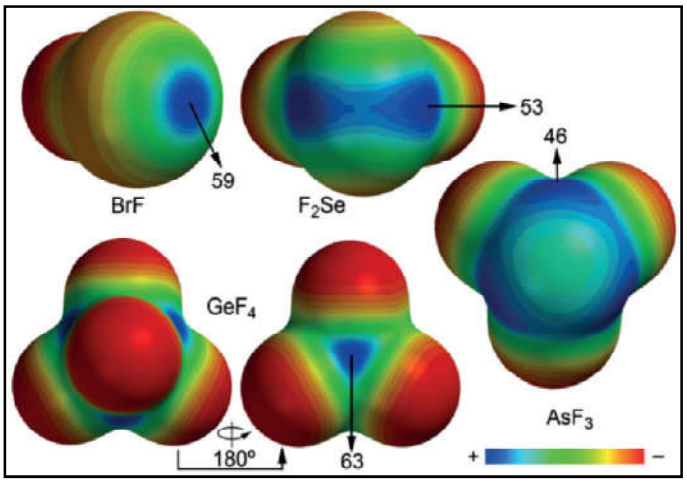

Figure 1.9 Molecular electrostatic potential (kcal/mol) of representative σ-hole halogen (BrF), chalcogen (SeF2), pnictogen (AsF3) and tetrel (GeF4) bonding interactions.

The magnitude of the electropositive potential as well as the steric environment of the σ-hole can influence its ability to act as electron-deficient host for an electron-rich guest molecule. The value of MEP at the σ-hole is similar in representative compounds of the same row (**Figure 1.9**, BrF, SeF_2, AsF_3 and GeF_4), the σ-holes are sterically more accessible with lower valence, i.e.: BrF>SeF_2>AsF_3>GeF_4. This steric hindrance is particularly relevant in the case of carbon, which is the smallest tetrel atom.

Thus, in a sp^3-hybridised electron-deficient C atom, such as C_2F_6 (**Figure 1.10**), there is only a very limited space available for the electron-rich guest molecule to nest itself for molecular association. In small rings such as hexafluorocyclopropane (C_3F_6, **Figure 1.10**), the σ-hole on C is more exposed due to the small FCCF dihedral angle.

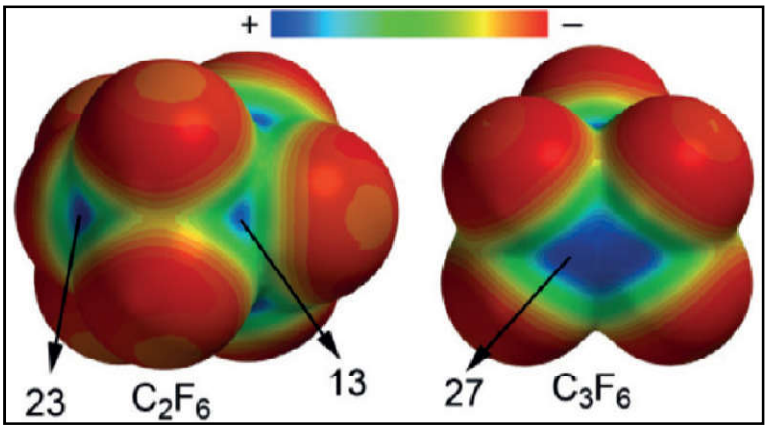

Figure 1.10 Molecular electrostatic potential surface (kcal/mol) of representative σ-hole (tetral bonding) involving carbon atoms in hexafluoroethane (left) and hexafluorocyclopropane (right).

1.2.8 π-hole Interactions

A π-hole can be described as the region of positive electrostatic potential obtained on an (partially) empty π* (anti-bonding) orbital, usually located in a perpendicular direction to the molecular framework. π-hole interactions can be classified into other subclasses depending on the nature of the electron-rich partner and the characteristics of the molecular fragment. Politzer *et al.*[52c] have introduced the term π-hole to describe the depletion of charge density of unoccupied π-orbitals on the central atom in SO_2 and related molecules. Grabowski has introduced the term *triel bonding* for Group 13 elements of the periodic table involved in such interactions.[58] This type of π-hole interaction has the electron depletion region located on a single atom (like σ-holes) and usually termed in the literature using the name of the group, for example pnictogen/chalcogen π-hole interactions.[59]

Figure 1.11 represents the MEP surfaces of four representative planar molecules where the π-hole is located over the central atom belonging to the second (F_2CO and FNO_2) or third (F_2SiO and FPO_2) row of the periodic table. The π-hole is found to be more accessible (more extended) in heavier (typically also larger) atoms (**Figure 1.12**).

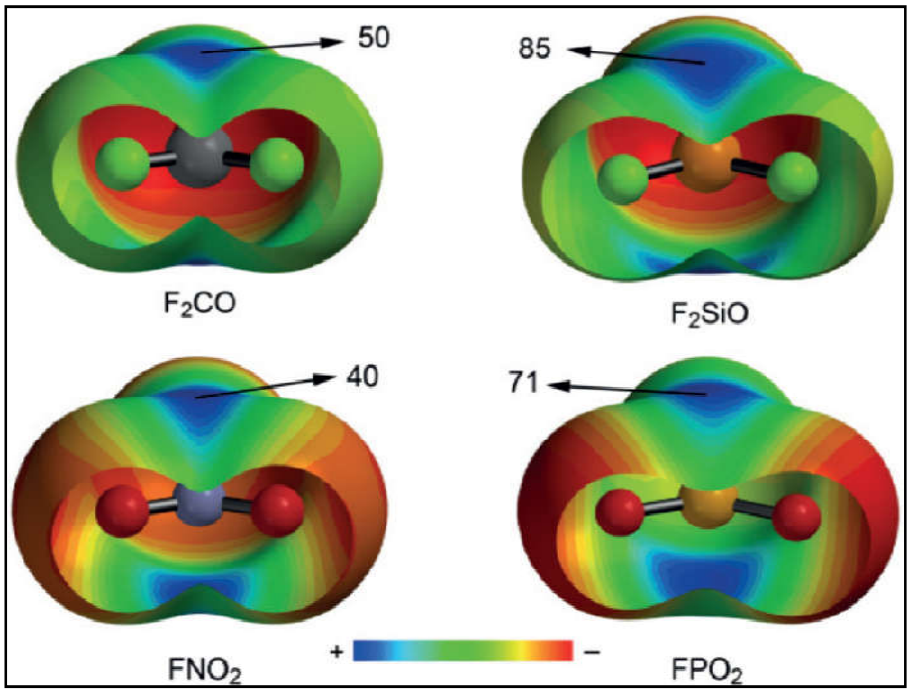

Figure 1.11 Molecular electrostatic potential of representative tetrel (F_2CO and F_2SiO), and pnictogen (FNO_2 and FPO_2) π-hole bonding interactions. Energies at the π-holes are given in kcalmol^{-1}.

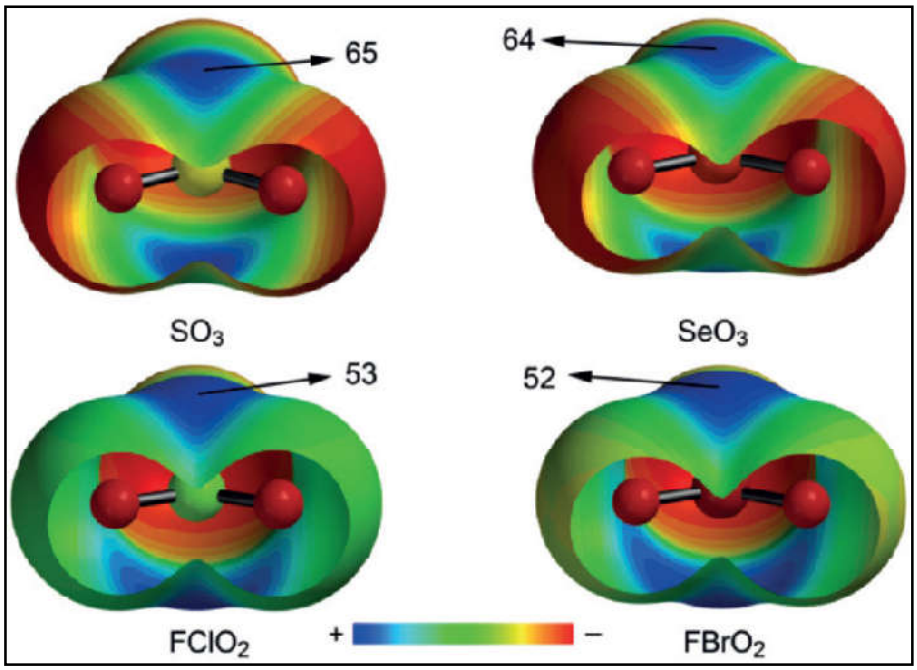

Figure 1.12 Molecular electrostatic potential of representative chalcogen (SO_3 and SeO_3) and halogen ($FClO_2$ and $FBrO_2$) π-hole bonding interactions. Energies at the π-holes are given in kcalmol^{-1}.

1.2.9 Anion–π and Lone Pair–π Interactions

Anion–π interaction (**Figure 1.13**) can be described as the non-covalent interaction between an anion and an electron deficient aromatic ring.[60] Berryman *et al.* have characterized the anion-π interaction with anion to ring distances less than the sum of the van der Waals radii of the participating atoms and the position of the anion to ring centroid should be perpendicular to the plane of the aromatic ring.[61]

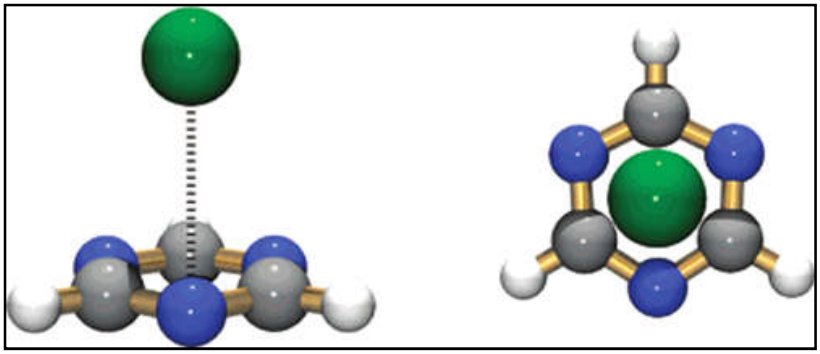

Figure 1.13 Anion-π interactions involving Cl^- and triazine (left); on top representation of the anion-π interactions (right).[62]

Anion–π interactions play an important role in the fields of medicine, environmental chemistry, chemical and biological processes[63] and metal-organic supramolecular assemblies.[64] The π-cloud on an aromatic ring is readily polarized by an anion. This induced polarization can also exhibit permanent quadrupole moment perpendicular to the ring plane.[65] The anion can then interact with this induced dipole. This polarization contribution to the total interaction energy of anion–π interaction should be substantial.[66] It can be expected that a more electron deficient aromatic ring tends to display stronger binding to anions. Furthermore, the presence of heteroatoms in aromatic rings can polarize the π-electron density; thus incorporating sufficient π-acidity to the rings. Further polarization in the rings can be observed due to the coordination of the rings to metal ions. The influence of metal coordination to heteroaromatic rings on the energetics of anion–π interactions has been analyzed in the literature.[67] Schottel and his coworkers have reported an interesting symmetrical anion–π interactions involving $[SbF_6]^-$ anion and six tetrazine rings in $[Ag_2(bptz)_3][SbF_6]_2$ [where, bptz = 3,6-bis(2′-pyridyl)-1,2,4,5-tetrazine] having anion to ring centroid distance of 3.265(3) Å (**Figure 1.14**).[68]

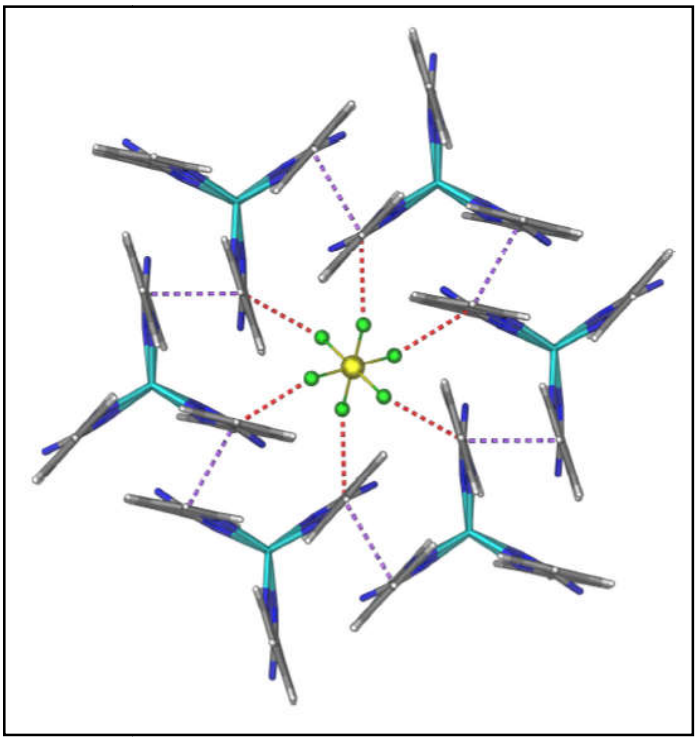

Figure 1.14 Anion-π interactions between $[SbF_6]^-$ anion and six tetrazine rings in $[Ag_2(bptz)_3][SbF_6]_2$.[68]

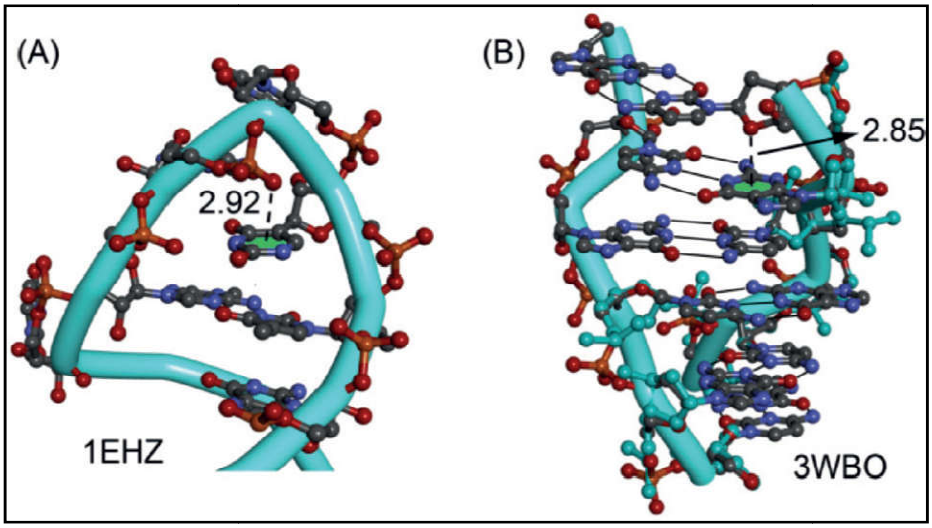

Figure 1.15 Short lp–π interaction (indicated as dashed line) in the Z-DNA (PDB ID: 3WBO); Distance in Å.

The attractive interaction between a lone pair of electron and the electron-deficient π-conjugate of an extended aromatic system is known as the lone pair (lp)–π interaction. The first experimental reports of lp–π interactions involves the X-ray

structure of Z-DNA (**Figure 1.15**).[69] Gamez *et al*.[70] have explored numerous lone-pair–π interactions involving electron-rich atoms such as halogens, oxygen and nitrogen with electron deficient aromatic centres having lone pair-centroid of the aromatic ring distances of less than 4 Å. The crystal structure of bis(4,4′-dichloro-2,2′-iminodibenzoic acid reveals lone-pair–π interaction[71] involving chlorine atom as shown in **Figure 1.16**.

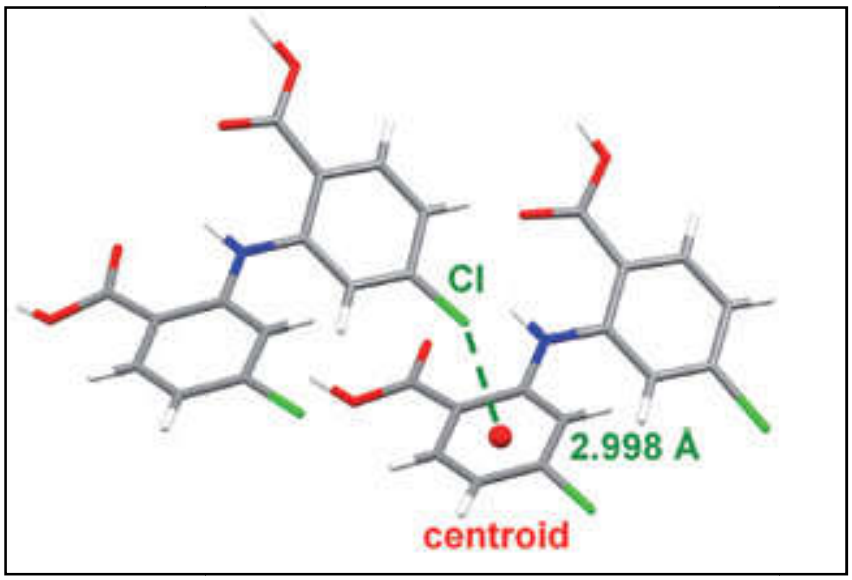

Figure 1.16 Lone-pair-π interaction in the crystal structure of bis(4,4′-dichloro-2,2′-iminodibenzoic acid.[71]

1.3 Molecular Recognition and Self-Assembly

The construction of supramolecular architectures involves two important and nearly synonymous processes[72] *viz*. molecular recognition and self-assembly. Molecular recognition is a process in which a molecule can utilize its functionalities to interact with other molecules in a well-defined and precise manner via intermolecular forces.[73] The concept of molecular recognition was described in 1894 by Emil Fischer in his lock-and-key theory.[74] In Fischer's original idea, molecular recognition can be compared to the complementarity of a lock and a key. The lock is like the molecular receptor and the key the substrate being recognized, thereby forming a receptor-substrate supramolecular complex. This simple idea emphasizes the necessity of complementarity between the donor and acceptor involving two chemical moieties in the process of recognition.

Molecular recognition plays an important role in the synthesis of bio-macromolecules[75] which is responsible for life in both prokaryotes and eukaryotes. It has also significant contribution in the double helical structure of DNA. The DNA bases adenine, thymine, guanine and cytosine are all polar aromatic N-heterocycles, having elements for molecular recognition.[76] A purine base (adenine = A or guanosine = G) specifically recognizes and interacts with a complementary pyrimidine base (thymine = T or cytosine = C) through hydrogen bonding interactions. This gives rise to A-T and G-C pairs, which stack along each strand of the DNA helix showing molecular recognition (**Figure 1.17**).

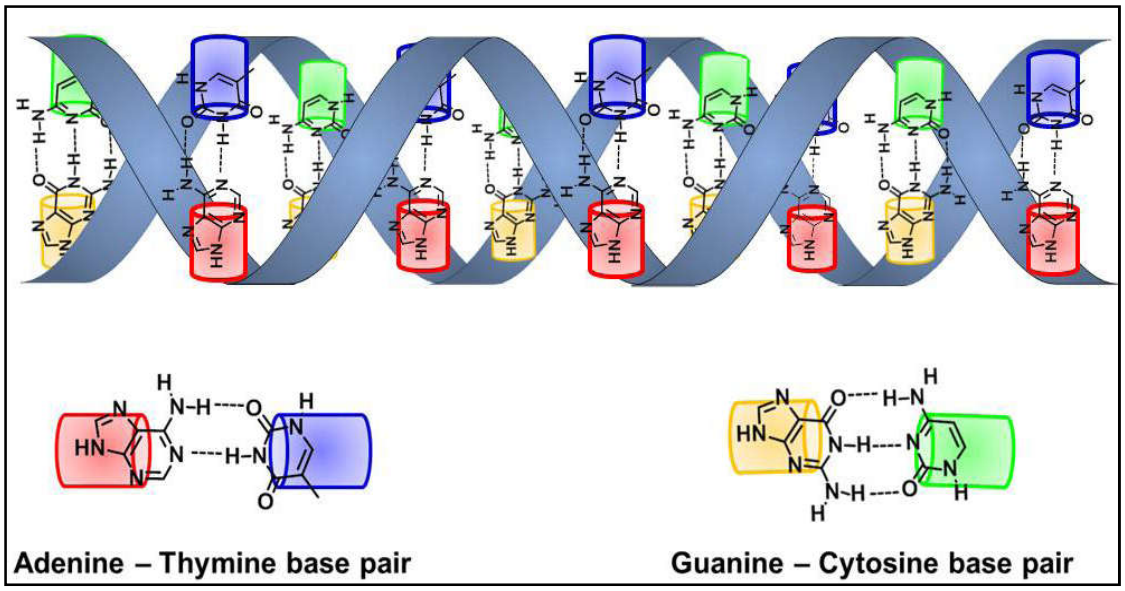

Figure 1.17 Molecular recognition in the double helical structure of DNA.

Self-assembly[77] is an integral process which plays a key role in the formation of desired supramolecular network architectures. Although there are many definition for self-assembly[78], the definition by George Whitesides is the most appropriate one, which defines self-assembly as "*the spontaneous assembly of molecules into structured, stable, non-covalently joined aggregates*" (**Figure 1.18**).[79] Self-assembly processes are extensively involved in supramolecular chemistry to construct complex structures and architectures, such as polygons, helicates, cages, polyhedra, rotaxanes, catenanes, and knots.[80] Self-assembly also plays a vital role in the stabilization of metal organic frameworks (MOFs) and covalent organic frameworks (COFs).[81]

Compared to typical covalent bonds (40-100 kcal/mol), the strengths of individual van der Waals interactions that are involved in self-assembly processes are very weak (0.1-5 kcal/mole). Therefore, for achieving acceptable stability for such self-assembled systems, the molecular associations must involve a large number of these weak non-covalent interactions. Such a self-assembled aggregate involving weak non-covalent interactions in large numbers in the crystal structures result in thermodynamically favourable structures. A self-assembled molecular aggregate has unique properties which are different from those of the molecular subunits from which it is constructed. The individual subunits contain all the information necessary for forming a self-assembled structure and bind cooperatively to give the most stable structure. The process of self-assembly is a reversible process and this makes the final structure capable of eliminating any mismatched molecular subunits.[82]

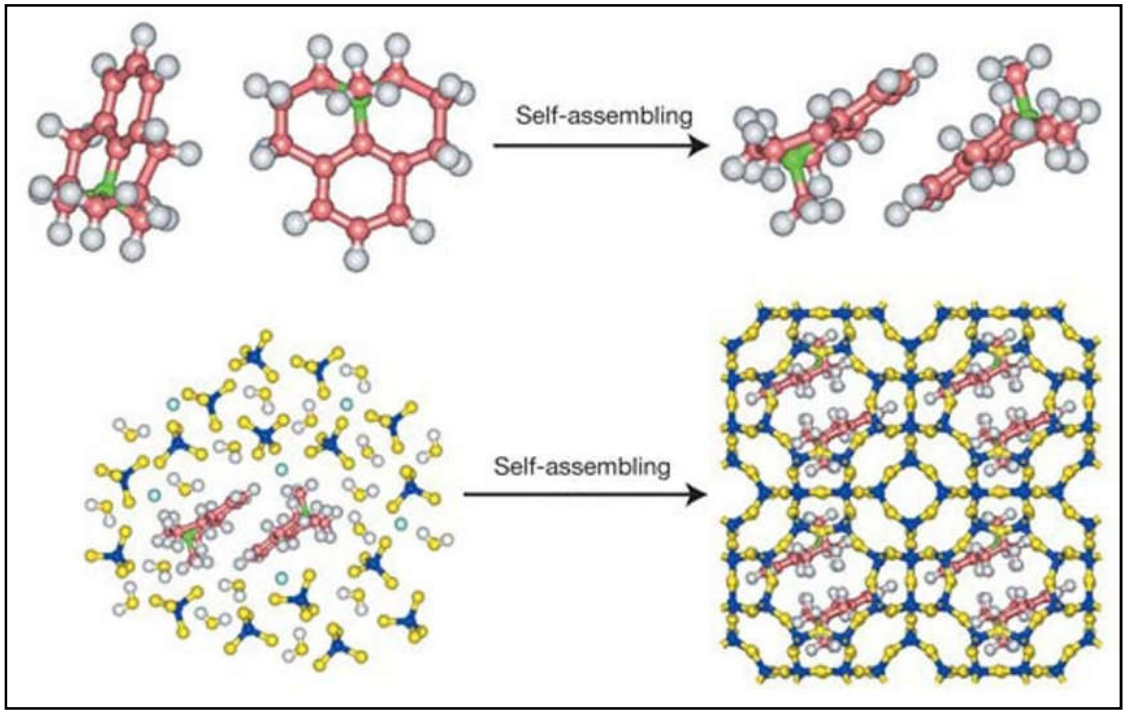

Figure 1.18 Formation of the zeolite structures from the supramolecular self-assembling of the organic structure-directing agents (OSDA). Here, 4-methyl-2,3,6,7-tetrahydro-1H,5H-pyrido quinolinium hydroxide was used as the OSDA.

1.4 Theoretical Methods for Studying Non-covalent Interactions

To understand the roles of non-covalent interactions in various chemical and biological fields, a proper fusion of experimental and theoretical studies is of utmost

importance. Various theoretical approaches *viz*. density functional theory (DFT), molecular electrostatic potential (MEP), non-covalent interaction (NCI) method, quantum theory of atoms in molecules (QTAIM), symmetry-adapted perturbation theory (SAPT) etc. are often employed to quantify non-covalent interactions. Various softwares *viz*. Gaussian[83], Abinit[84]; NCIPLOT[85]; AIMAII[86] and SPARTAN[87] have been developed to visualize the non-covalent interactions in molecular systems.

1.4.1 Density Functional Theory (DFT)

The quantum mechanical wave function, in principle, contains all the information about a given system. In case of an electron in a simple 2D box or even a hydrogen atom, the Schrödinger's equation can be solved exactly to get the wave function of the system. This can then be used to determine the allowed energy states. For an N-body system, however, it is not possible to solve the Schrödinger's equation. Therefore, some approximations must be considered to solve the equation. Density functional theory (DFT) is nothing but a method to obtain an approximate solution to the Schrodinger equation for N-body systems.[88] In DFT, the number of the degrees of freedom of a system is reduced as far as possible by the most basic approximation, called the Born-Oppenheimer approximation.[89] It is one of the most widely used methods for *ab-initio* calculations of the structure of atoms, crystals, molecules, surfaces, and their interactions. The DFT method can be applied to treat such systems with sufficiently high accuracy.

The density functional theory is based on two fundamental mathematical theorems of Kohn and Hohenberg and the derivation of a set of equations proposed by Kohn and Sham.[90] According to the first Hohenberg-Kohn theorem, the ground-state energy of a chemical system obtained from the Schrodinger's equation is considered to be a unique functional of the electron density. The second theorem is related to an important property of the functional which states that the electron density which minimizes the energy of the overall functional is the true electron density that corresponds to the full solution of the Schrodinger's equation.

The advantage of DFT is that the attention can be focused on the electron density of a system rather than on its wave function, which is the case in the usual Schrodinger equation method. The electron density is a function of space and time and

the use of electron density rather than wave function as the fundamental property for a system significantly increases the speed of the calculation. The many-body electronic wave functions are function of 3N variables (the coordinates of all the N atoms in the system); whereas, the electron density is a function of only three variables (x, y, z). It is evident from the Hohenburg-Kohn theorem that the electron density of any system provides all of its ground-state properties and thus, the total ground state energy of many-electron systems can be assumed to be a functional of the electron density. So, if the electron density functional of a many-electron system is known, the total energy of the system can be determined.

DFT calculations is being thoroughly used to solve problems in atomic and molecular physics, which include the calculation of ionization potentials,[91] vibration spectra, the study of chemical reactions, the structure of biomolecules[92] and the nature of active sites in catalysts[93] as well as problems in condensed matter physics, such as lattice structures,[94] phase transitions in solids[95] and liquid metals.[96] DFT study of the metal-organic frameworks with potential bioactive applications is a very useful method to explore their structural parameters in detail and to identify how the molecule interacts with each other or with a receptor bio-molecule.[97] Structure optimization of complex supramolecular networks usually provides the basis for the deeper understanding of the complicated system's functionality which is often difficult to obtain experimentally.[98]

The search for better correlation between experimental observations and DFT simulations has even led to the incorporation of empirical or semi-empirical parameters into the functionals to enhance their performance.[99] Various methods have been developed for the treatment of dispersion corrections in the non-covalent interactions. including treatments with specialized functionals, such as BMK and the M05/M06 series; dispersion corrected functionals such as B97D and double hybrid functionals, such as B2PLYP.[100] Grimme *et al* have designed the functionals in the DFT-D family (DFT-D2, DFT-D3 and DFT-Dx);[101] which are the most widely-used dispersion corrections nowadays due to their relative accuracy, simplicity and particularly its widespread implementation in popular software packages such as Gaussian. The B3LYP functional in DFT-D family has generally been the method of choice for hydrogen bonding interactions in self-assembled systems and in bio-molecules such as peptides.[102]

1.4.2 Molecular Electrostatic Potential (MEP)

Molecular electrostatic potential (MEP) is an important computational tool for predicting the reactive behaviour of various sites of a chemical system.[103] Qualitative investigations of the electrostatic potentials on the surfaces of a molecule can give idea about the regions of positive and negative electrostatic potentials which promote or inhibit non-covalent interactions during self-assembly processes.[104] Thus MEP analysis provides a good indication in assessing the molecules' reactivity towards positively or negatively charged reactants. Over a period of time, a quantitative approach has also been developed, which provides the detailed characterization of the molecular surface electrostatic potential, $V_S(r)$, in terms of certain statistically defined quantities.[105] Two site-specific statistical quantities are the most negative and most positive values of $V_S(r)$, designated respectively as V_S^{min} and V_S^{max} (*V_S^{min} and V_S^{max} are the extreme minima and maxima of the molecular electrostatic potential respectively implying the most negative and positive regions of a complex/molecule*).

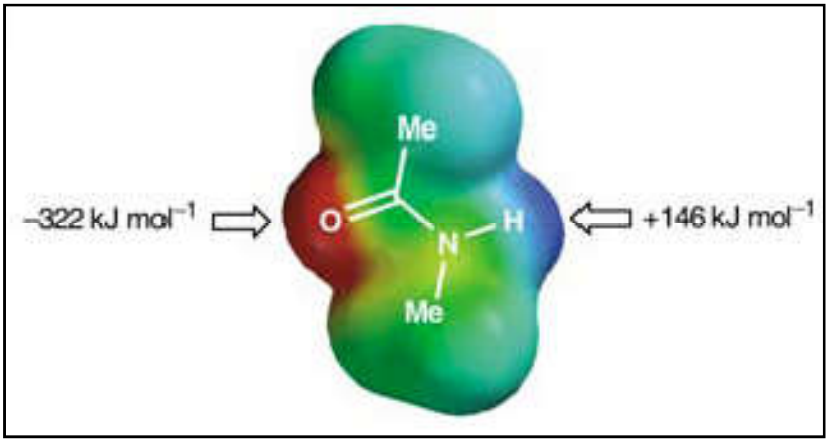

Figure 1.19 Molecular electrostatic potential surfaces plotted on the van der Waals surface of N-methyl acetamide. Positive regions are shown in blue (+146 $kJmol^{-1}$); negative regions are shown in red (–322 $kJmol^{-1}$) and green is neutral. The maximum in the electrostatic potential, V_S^{max}, lies over the NH group, and the minimum, V_S^{min}, lies over the carbonyl oxygen atom: the two primary hydrogen-bonding sites in the molecule.[106]

In most cases, for the electrostatic potential on the van der Waals surface of a molecule (*the van der Waals surface of a molecule is an abstract representation or model of that molecule, illustrating where a surface might reside for the molecule based on the van der Waals radii for individual atoms*), the maximum is usually located near a

hydrogen atom and the minimum is located over a lone pair or an area of π-electron density (**Figure 1.19**). Therefore the pair wise interactions between these maxima and minima from neighbouring molecules can dominate the electrostatic interactions. So, from the MEP surface analysis, we may generally identify various non-covalent interactions including H-bonding regions of chemical species. In MEP, the term "*heap*" is used to describe the most negative value of the MEP, while the most positive region is represented as "*hole*".[107] These holes and heaps can give rise to non-covalent interactions during molecular associations in supramolecular assemblies. Tomasi *et al*. pioneered the application of MEP for understanding intermolecular interactions.[108]

1.4.3 Non-covalent Interaction (NCI) Method

Yang and co-workers have introduced the non-covalent interaction (NCI) method[109], which maps the non-covalent interaction zone in real-space regions. It is based on a 2D plot of the electron density (ρ) and the reduced density gradient (s), defined as:

$$s = \frac{1}{2(3\pi^2)^{1/3}} \cdot \frac{|\nabla\rho|}{\rho^{4/3}}$$

The combination of *s* and ρ partitions the real space into bonding regions; (a) high-*s* and low-ρ corresponds to non-interacting density tails; (b) low-*s* and high-ρ corresponds to covalent bonds and (c) low-*s* and low-ρ corresponds to non-covalent interactions.

At low density regions, $\rho^{4/3}$ (denominator) becomes very small and tends to zero, thereby increasing the *s* value exponentially to infinity. Similarly, at high density regions, higher values of $\rho^{4/3}$ cause the steady decrease in *s* value. The reduced density gradient (*spatial variation of electron density over an area*) between the interacting atoms of neighbouring molecules undergoes a crucial change when a weak inter- or intra-molecular interaction takes place, thereby producing density critical points between the interacting molecules. Each density critical points provide a trough (**Figure 1.20**) in the s(ρ) plot. In real space, the density critical points representing the non-covalent regions during supramolecular associations give rise to this feature and are denoted by green isosurfaces.

The analysis of the electron density in the troughs reveals their origins, *viz*. steric interactions, hydrogen bonds, etc. However, both attractive and repulsive interactions

(i.e. hydrogen-bonding and steric repulsion) appear in the same region of density/reduced gradient space. They are distinguished by the sign of the second density Hessian eigen value (λ_2).[110] For bonding interactions, the electron density is locally accumulated with respect to the plane perpendicular to the bond path and $\lambda_2 < 0$. For non-bonding interactions or steric clashes, which produce density depletion, $\lambda_2 > 0$. Finally, the van der Waals interactions are characterized by a negligible density overlap, thereby giving $\lambda_2 \leq 0$. Thus, while interaction strength can be assessed by the density itself, analysis of the sign of λ_2 distinguishes different types of weak interactions.

Kashyap *et al*. have used NCI-plot analysis (**Figure 1.21**) to explore the nature and extent of supramolecular interaction between the aromatic surface of benzene and hydrogen bond donors as well as lone pair containing molecules.[111] The large green isosurfaces for the interaction between benzene and water as well as ammonia corroborate the fact that the H atoms of both water and ammonia are involved in non-covalent interaction with the π cloud of the benzene ring. However, in case of HF, the interaction between HF and the aromatic ring is through lone-pair-π interaction.

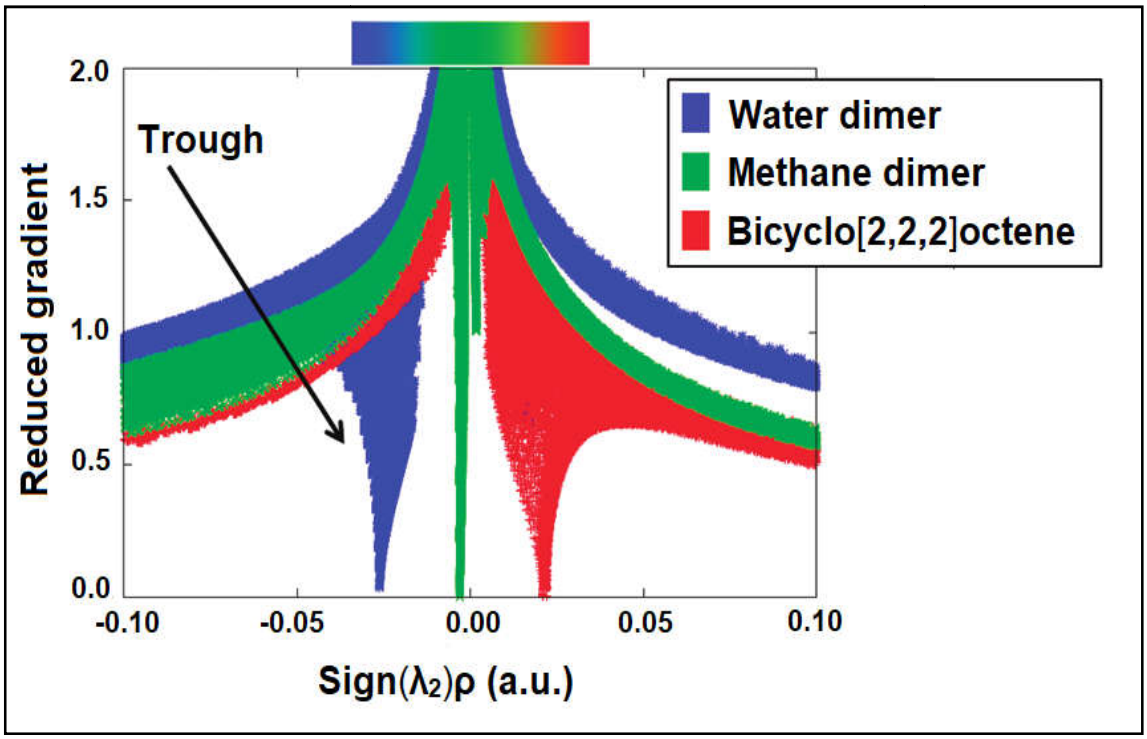

Figure 1.20 Overlapping troughs of water dimer, methane dimer and bicyclo[2,2,2]octene in s(ρ) plots.[109]

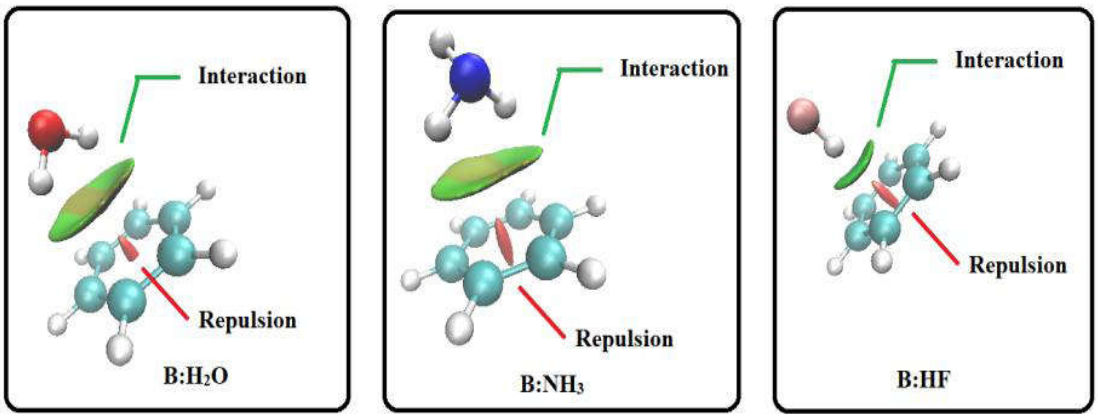

Figure 1.21 NCI-plot of some representative molecules involving the aromatic surface of benzene (B).[111]

1.4.4 Quantum Theory of Atoms in Molecules (QTAIM)

Bader's quantum theory of atoms in molecules (QTAIM)[112] analyzes the topology of electron density in a molecule. This topology is dominated by the electron-nuclear force, causing the electron density (ρ) to exhibit maxima or minima or a saddle point in space between the interacting systems which are referred to as critical points (CPs). QTAIM is one of the appropriate methods for analyzing different intra- and intermolecular interactions, since their properties are expressed as functions of a real electron density of a system. The topological properties of electron density and its derivatives are found to be immensely useful in defining the concept of the bonding through bond paths and bond critical points (BCPs). The topology of the electron density (ρ) yields a reliable mapping of the molecule and is effectively described by a set of critical points (CPs); the CPs of the electron density distribution is associated with atomic nuclei, bonds, rings and cages.

In order to have a deeper insight into the nature of the topological atoms, the concept of gradient paths (GPs) has been introduced. **Figure 1.22(a)** shows the partitioning of the gradient paths of the four atoms (C, H, O and F) of HFC=O molecule into four topological regions separated by three bold black curves. **Figure 1.22(b)** represents the bond critical points (BCP) in HFC=O molecule (black squares) where more than one GP meet with the property $\nabla\rho = 0$ i.e. change in electron density associated with the GPs is zero.

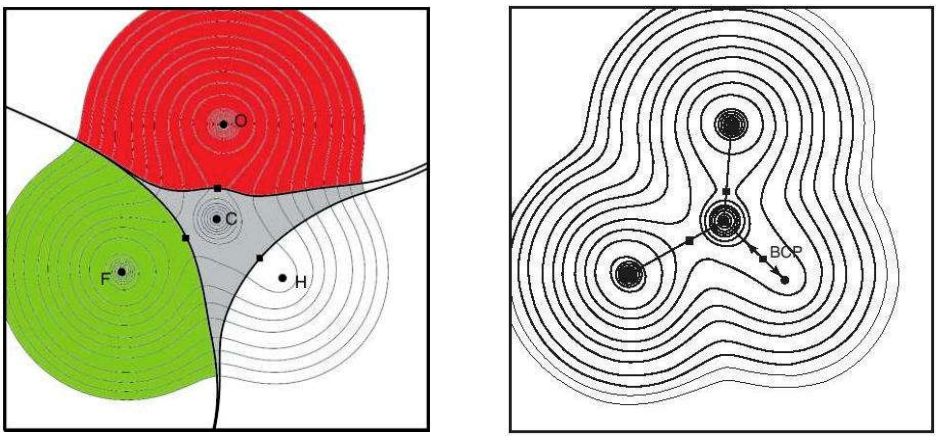

Figure 1.22(**a**) Partitioning of HFC=O molecule into four topological atoms; (**b**) bond critical points (BCP) in HFC=O, one explicitly marked by the BCP and lies in between C and H.

Usually, the non-covalent interactions studied by QTAIM analysis can be classified into three groups. The first one is related to the interactions in σ orientation (such as H-bonds), which is basically explained by a bond critical point (BCP).[113] When there is a hydrogen bonding interaction, bond critical points appear between the hydrogen atom and the acceptor atom. The second group implies interactions with aromatic rings such as anion-π, cation-π or π-π stacking, defined by a ring critical point (RCP). The last group implies the interactions of electron rich atoms/ions with a cage formed by several aromatic rings and defined by a cage critical coint (CCP). Greater the electron density (ρ) values at the critical points, the stronger the non-covalent interactions.

In solid state analysis, NCI plots (*vide supra*) have several advantages over traditional QTAIM critical point maps, such as (i) The numerical and algorithmic problems in locating exactly the position of the density critical points are avoided; (ii) The transition from bonding to non-bonding cases is gradual instead of catastrophic; (iii) The NCI regions provide information about the extent of the interaction in real space.

1.4.5 Symmetry-Adapted Perturbation Theory (SAPT)

In recent times, non-covalent interactions have gained immense interest in research fields because of their potential applications in biological and material

chemistry.[114] Two main approaches have been usually used in quantum chemistry for the calculation of non-covalent interaction energies *viz*. supermolecular and perturbative approaches. According to the supramolecular approach, the difference between the total energy of the whole complex and the sum of the energies of each isolated monomers is considered to be the interaction energy.[115] Whereas, in case of perturbative approaches, the interaction energy of the complex is directly computed as a perturbation to the Hamiltonian of the individual monomers.[116] Such an approach is known as the Symmetry-Adapted Perturbation Theory (SAPT) and widely used in theoretical chemistry to evaluate the interaction energy.[117] In SAPT, the interaction energy is calculated as a sum of perturbative corrections, where each correction results from a different physical effect. Similar to dispersion correction (*vide supra*), perturbative corrections are performed in SAPT to correlate experimental and theoretical observations. Thus, SAPT provides the total interaction energy in terms of several physical components such as electrostatics, exchange, induction, and dispersion.[118] Electrostatic interaction energy includes coulombic multipole-multipole-type interactions along with the interpenetration of charge clouds. Exchange-repulsion is the repulsive force arising due to the overlap of the wave functions of neighbouring monomers. Induction arises between the adjacent monomers due to overlap of the individual electric fields of the monomers and charge transfer between them. Dispersion is the attractive force which results from the dynamical movement of electrons of one monomer with those of the neighbouring monomer. This type of separation of the interaction energy of the complex molecules into various distinct physical components is the unique characteristic of SAPT, which provides a key advantage over the supermolecular approaches.[119]

1.5 Crystal Engineering

Crystal engineering[120] has emerged as an important research area in supramolecular chemistry, which deals with the single crystal X-ray structure of the compounds. It can be defined as "*the understanding of intermolecular interactions in the context of crystal packing and in the utilization of such understanding in the design of new solids with desired physical and chemical properties*".[121] Therefore, crystal engineering can be regarded as the "*design of crystal structures*"[122] using various non-covalent supramolecular contacts.

In the late 1980s, crystal engineering started to evolve from a hypothesis to the scientific discipline focusing the design of organic solids with desired properties and structures at the molecular level using supramolecular synthons (*vide infra*).[123a, 123b] The initial research focused purely on organic-based systems, where supramolecular forces, hydrogen bonding in particular, were exploited to generate solid-state architectures.[123c] With the enhancement in the study of metal based inorganic systems, this field has developed significantly due to wide range of geometries available for transition metal complexes.[124]

The above definition[121] of crystal engineering involved three stages, *viz*. structure; design and property (**Figure 1.23**). In the initial stages, the subject was limited with the study of molecular organization in terms of intermolecular interactions.[125] Later on, a systematic protocol in terms of a logic driven methodology was introduced to achieve desired architectures, where supramolecular synthons were used as a facilitating concept.[126] Property of the crystals was not explicitly targeted in this phase of crystal engineering. However, when a property was obtained, it was optimized by minor changes at the molecular level, which in turn results in the changes at the crystal level. Recently, researchers are exploring targeted solid state properties or property engineering of solids that can take the crystal engineering research to higher dimension.

The literature provides structure inputs to construct structural models so as to obtain the property of the crystals (*first stage of crystal engineering*). This is followed by design strategies, which use supramolecular synthons or any other protocol to obtain the targeted structure (*second stage of crystal engineering*). In the development of crystal engineering, these two stages could be termed as generations[127] (**Figure 1.23**).

Over the last 50 years, the first two generations have been well exploited by various research groups. *The third generation of crystal engineering* has evolved with some recent discoveries of property engineering of organic and metal-organic crystals which are restricted to mechanical properties till now.[128] Crystal engineering of elastic crystals is not an easy task; but in recent years much attention has been paid to grow single organic or metal-organic solid crystals with flexible elastic behaviour.[129] A π-conjugated organic crystal *viz*. (Z)-2-(4-(((E)-2-hydroxy-5-methylbenzylidene)amino)phenyl)-3-phenylacrylonitrile has been recently reported

which is found to exhibit elasticity not only at room temperature but also at low temperatures (77 K) in liquid nitrogen.[130] Kenny *et al*. have reported the dramatic change in magnetic properties of an elastically flexible crystal *viz*. $[Cu(acac)_2]$ when the crystal is bent.[131] Very recently, Bhattacharya and his research group have reported the first elastically-flexible coordination polymer *viz*. $[Zn(\mu\text{-}Cl)_2(3,5\text{-dichloropyridine})_2]_n$ which is flexible over two crystallographic faces.[132]

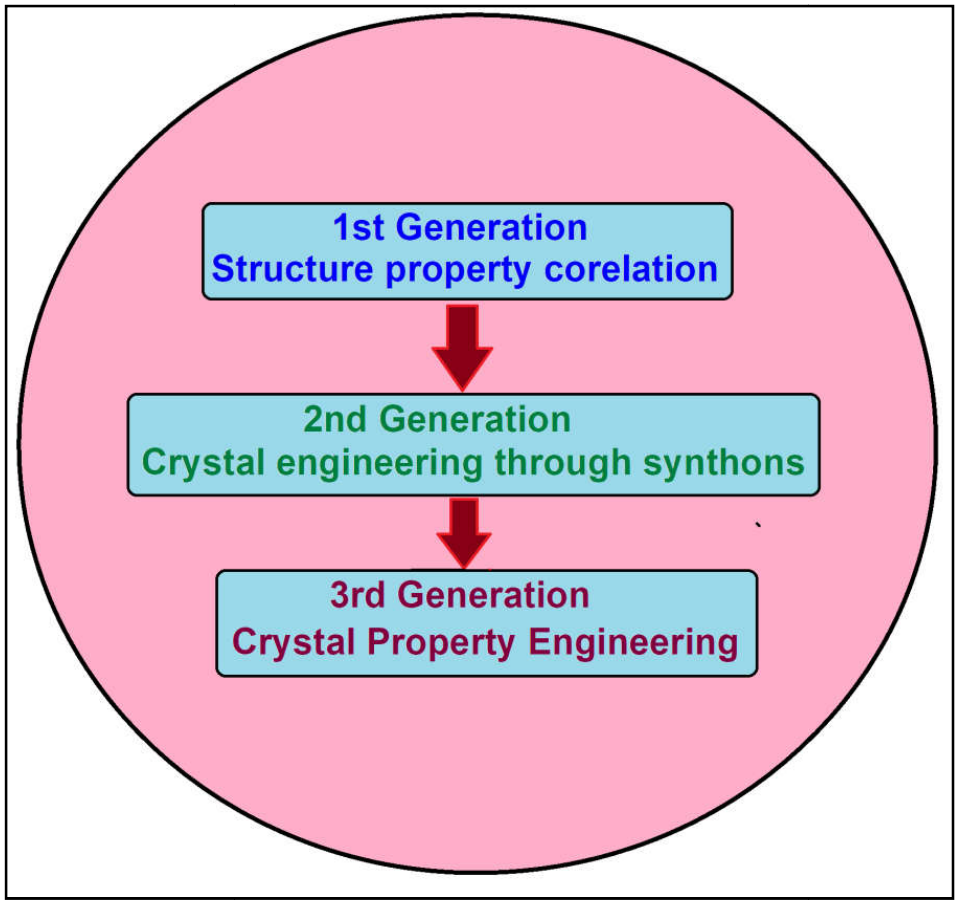

Figure 1.23 Development of crystal engineering through different generations.

Crystal engineering represents an opportunity to generate new solid state architectures via self-assembly processes. Moreover, the diversity of the physicochemical properties associated with engineered materials can be exploited in many areas as demonstrated by co-crystals, which have relevance to non-linear optics[133], host-guest chemistry[134], photographic materials[135], organic conductors[136], pharmaceuticals[137] and solid-state organic chemistry.[138]

1.6 Supramolecular Synthons

The crystal structures may be formally represented as network architectures, where the molecules are considered as the nodes and the intermolecular interactions are node connections.[139] The predictable self-assembly of molecules via supramolecular interactions in network architectures of various dimensions is very important in crystal engineering. Conventional strong hydrogen bonding interactions of the types O−H···O and N−H···O are the most commonly used supramolecular contacts for designing crystals, though weaker interactions such as C−H···O, C−H···N or even C−H···C also have prominent roles.[140] All these interactions are so directional that the orientation of the molecules in the solid state structure can be predicted with a reasonable degree of accuracy. A properly designed placement of functional groups in the molecular skeleton can facilitate such supramolecular interactions to generate what are called "*supramolecular synthons*".

In 1967, Corey first introduced the term "*synthon*" in the article entitled "*General Methods for the Construction of Complex Molecules*".[141] The term synthon as defined by Corey was traditionally used to represent key structural features in a target molecule for organic synthesis. Corey defined a synthon so generally and flexibly that even today it can be used with almost the same connotations in a supramolecular sense. As coined by Gautam Desiraju[142], "*Supramolecular synthons are structural units within supermolecules which can be formed and/or assembled by known or conceivable synthetic operations involving intermolecular interactions.*" In short, supramolecular synthons are spatial arrangements of intermolecular interactions, which play the same role in supramolecular synthesis as do the conventional synthons in molecular synthesis.

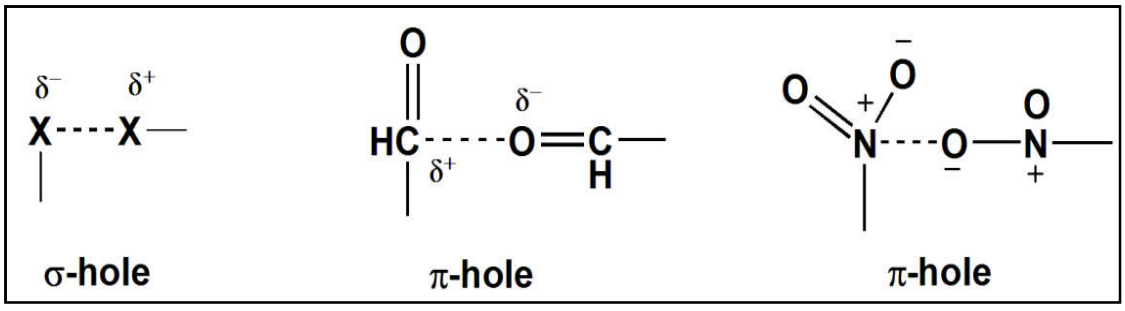

Figure 1.24 Supramolecular synthons involving σ- and π-hole interactions.

Recently, π-hole based synthon involving the π-cloud of the oxalate moiety has been reported in a oxalato bridged supramolecular ternary complex *viz*. $[Cu_2(\mu_2\text{-}C_2O_4)(phen)_2(H_2O)_2][Cu(phen)(male)(NO_3)]_2$ [where, phen = 1,10-phenanthroline, C_2O_4 = oxalate, male = maleate].[143] The π-hole interaction was further established energetically using DFT calculations and NCI plot analysis. Similarly, Jiwon *et al*. have reported a series of Se(II) compounds *viz*. 2^{Se}-BX_3 [where, X = Ph, F, Cl, Br, I and 2^{Se} = benzo-2,1,3-selenadiazole].[144] The structures of the compounds demonstrate the supramolecular dimerization through the $[Se\text{-}N]_2$ σ-hole supramolecular synthon via Se···N chalcogen bonding interactions. Similarly, carbonyl···carbonyl[145] and nitro···nitro interactions[146] are typical examples of such π-hole based synthons.

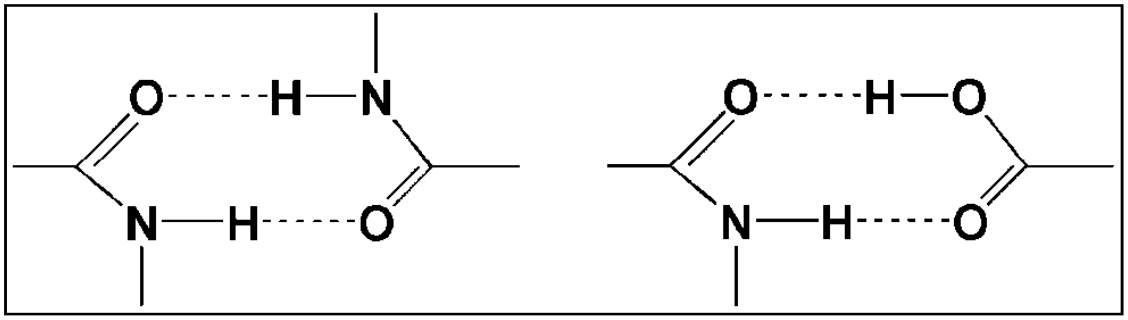

Figure 1.25 Amide homodimer synthon (left); amide acid hetero synthon (right).

In contrast to a molecular target involving covalent bonds, two common and distinct types of H-bonded synthons are observed in supramolecular architectures, *viz*. homosynthons and heterosynthons.[147] A homosynthon consists of two or more identical hydrogen bonding functional groups, whereas, a heterosynthon consists of two or more different, but complementary, hydrogen-bonding functionalities (**Figure 1.25**).

1.7 Metallosupramolecular Chemistry

In the field of supramolecular chemistry, metal coordination is considered as a "*non-covalent*" interaction, though it often possesses a strong covalent component in binding processes. This is not only applicable for the transition elements, but also for alkaline, alkaline earth or lanthanide metal cations. Electrostatic and dipole-dipole interactions are the main driving force responsible for these interactions. The branch of supramolecular chemistry involving metal coordination can be termed as

metallosupramolecular chemistry[148], which deals with metal ion directed self-assemblies of organic ligands.

It is well established that metal cations are particularly effective as synthetic tools. Amongst the intermolecular forces, metal-coordination is the strongest one, providing highly directional bonding and structural control. Metals are also excellent templates for the self-assembly of supramolecular architectures of various dimensions.[149]

Voda *et al*. have reported two mixed-ligand isostructural complexes involving 2,6-pyridinedicarboxylato ligand *viz*. $[Co_2(BIBP)(2,6\text{-}PDC)_2(H_2O)_4]$ and $[Ni_2(BIBP)(2,6\text{-}PDC)_2(H_2O)_4]$; [where, BIBP = 4,4′-bis(1-imidazolyl)biphenyl, 2,6-PDC = 2,6-pyridinedicarboxylate.[150] The common motif in them is the bridging nature of the neutral BIBP ligand between two metal ions and a metal chelating coordination of the dianionic 2,6-PDC ligand through the pyridine N atom and the carboxylate group.

Mistri *et al*. have reported two Cu(II) coordination complexes involving 2,6-pyridinedicarboxylato ligand *viz*. [Cu(2,6-PDC)(im)] and $\{[Cu(2,6\text{-}PDC)(2\text{-}ap)(H_2O)]\cdot 2H_2O\}$ [where, 2,6-PDC = pyridine-2,6-dicarboxylate; im = imidazole and 2-ap = 2-aminopyridine].[151] Both the complexes form hydrogen bonded 3D supramolecular network architectures in the solid state (**Figure 1.26**) which are further studied by computational tools. The compounds are reported to exhibit fluorescence activity in water-methanol solution at room temperature.

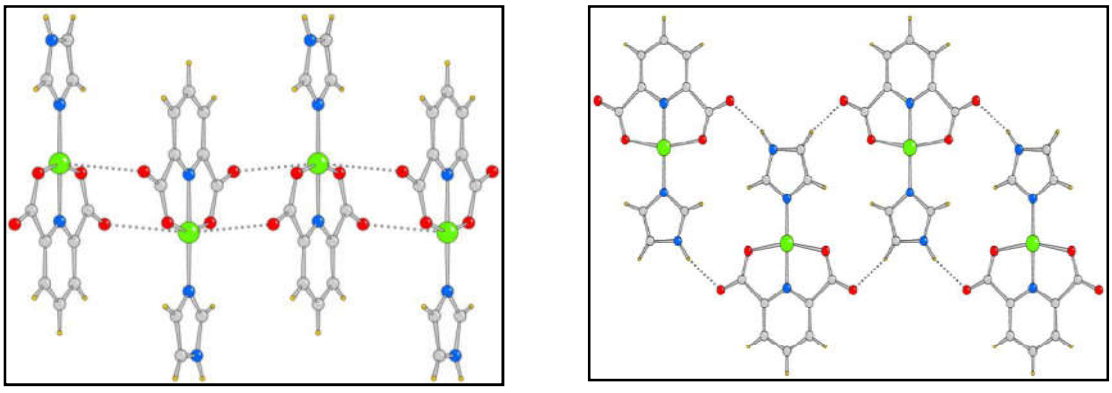

(**a**) (**b**)

Figure 1.26 Supramolecular polymeric architectures of (**a**) [Cu(2,6-PDC)(im)]; (**b**) [Cu(2,6-PDC)(im)] assisted by N–H···O and C–H···O hydrogen bonding interactions.[151]

S. C. Manna *et al*. have reported a centrosymmetric dimer of Cu(II) involving 2,5-pyridinedicarboxylato ligand *viz*. $[Cu(HL)(2,5\text{-}PDC)]_2$; [where 2,5-PDC = pyridine-2,5-dicarboxylate and HL = 2-([2-(piperazin-yl)ethylimino]methyl)phenol].[152] The lattice water molecules along with the protonated piperazinium fragment of the complex are involved in N–H···O, C–H···O and O–H···O hydrogen bonding interactions resulting in a 3D supramolecular network architecture. The cytotoxicity of $[Cu(HL)(2,5\text{-}PDC)]_2$ was determined by MTT [3-(4,5-dimethylthiazol-2-yl)-2,5–diphenyltetrazolium bromide] assay (*vide infra*) against human breast (MCF7) cancer cell lines.[152] The result reveals that the complex has a moderate anti-proliferation activity against MCF7 cells. Molecular docking (*vide infra*) of the complex (**Figure 1.27**) shows that it binds with DNA (PDB ID: 1BNA) through N–H···O hydrogen bonding interactions.[152]

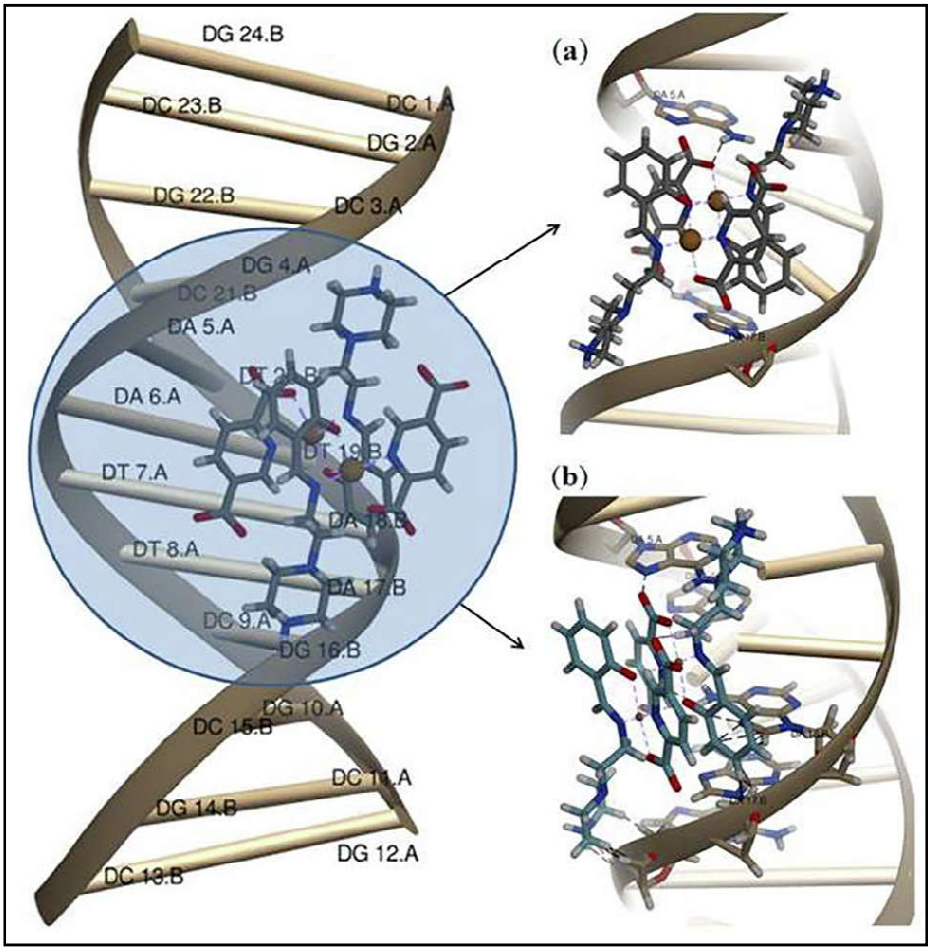

Figure 1.27 Molecular docking of $[Cu(HL)(2,5\text{-}PDC)]_2$ with DNA, showing the binding sites involving (**a**) hydrogen bonding and (**b**) intermolecular interactions.

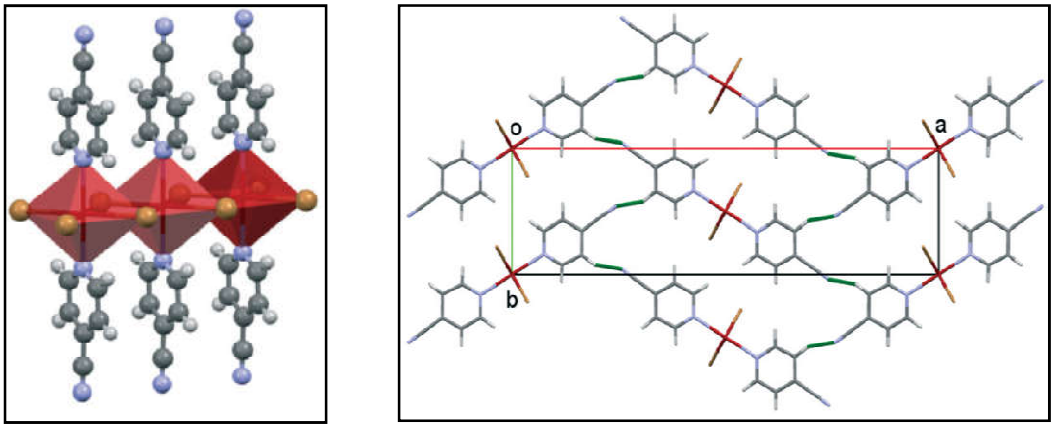

(**a**) (**b**)

Figure 1.28(**a**) Molecular structure and (**b**) the polymeric chain of $[FeBr_2(4\text{-}CNpy)_2]_n$.

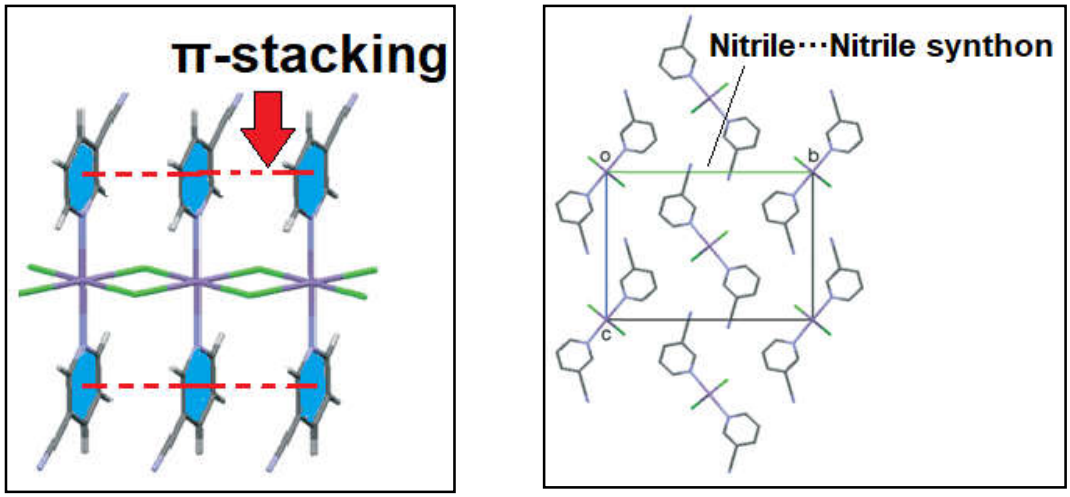

(**a**) (**b**)

Figure 1.29(**a**) Part of a $[MnCl_2(3\text{-}CNpy)_2]_n$ polymeric chain; (**b**) herringbone packing motif of $[MnCl_2(3\text{-}CNpy)_2]_n$. Hydrogen atoms omitted for clarity.

Heine *et al.*[153] have reported a series of new polymers of type $[MX_2(4\text{-}CNpy)_x]_n$ with M = Mn, Fe, Co, Ni, Cu, and Zn; X = Cl and Br; 4-CNpy = 4-cyanopyridine and x = 1 and 2. In all of them, the halogen atoms bridge two metal atoms, leading to infinite $[MX_2]_n$ chains (**Figure 1.28**). These 4-CNpy complexes were compared with the structures of the corresponding 3-CNpy counterparts. It was found that in the case of $[MCl_2(3\text{-}CNpy)_2]_n$ compounds; [where, 3-CNpy = 3-cyanopyridine and M = Mn, Fe, Co, Ni, Cu, Zn], the central metal ions are octahedrally coordinated by four chlorine

atoms and two 3-CNpy ligands, that coordinate to the central metal ion with N_{py} atoms (**Figure 1.29a**). In all the structures, the adjacent monomeric units are arranged in a herringbone packing motif assisted by the nitrile···nitrile synthons (**Figure 1.29b**). The cyano groups of neighbouring chains are orientated in the anti-parallel manner allowing stronger π-stacking interactions within the chain.

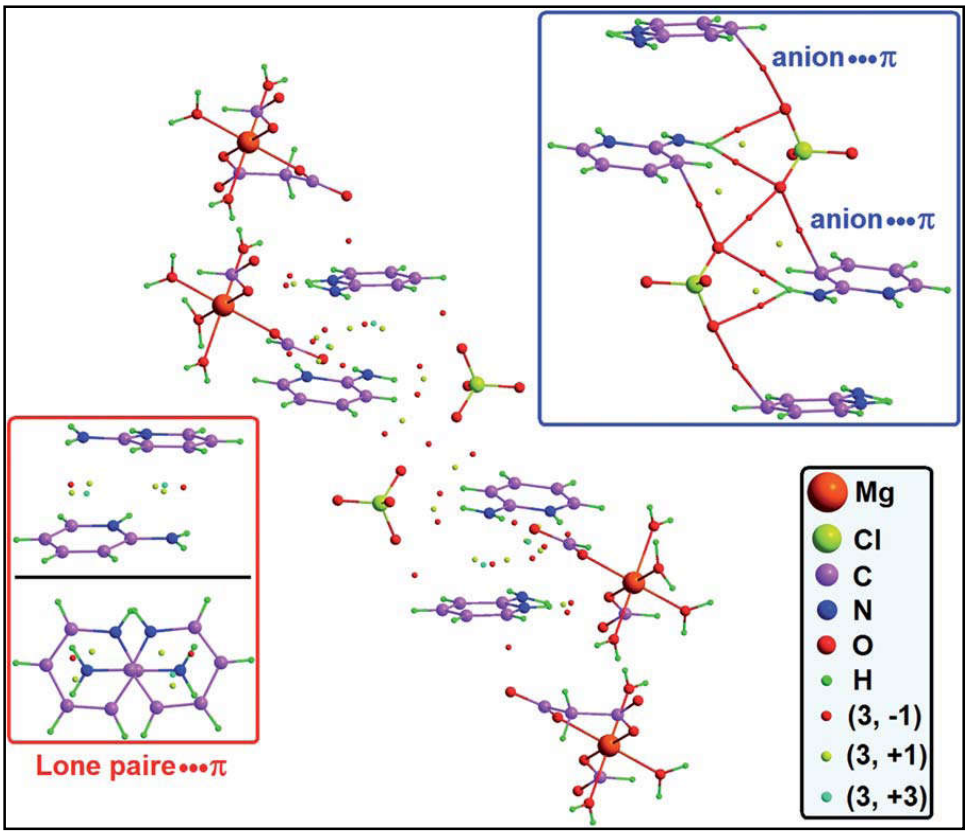

Figure 1.30 AIM analysis of a large fragment of $(C_5H_7N_2)_4[Mg(C_3H_2O_4)_2(H_2O)_2](ClO_4)_2$ showing the occurrence of hydrogen-bonds, lone pair···π, π-π, and anion–π interactions in its crystal packing.[154]

In the compound $(C_5H_7N_2)_4[Mg(C_3H_2O_4)_2(H_2O)_2](ClO_4)_2$ [where, $C_5H_7N_2$ = 2-aminopyridine, $C_3H_2O_4$ = malonic acid, ClO_4 = perchlorate], two perchlorate oxygen atoms are involved in anion–π contacts[154] with two different neighbouring aminopyridinium cations. The 2-aminopyridine ring is further involved in π-stacking over a neighbouring 2-aminopyridine molecule in a head-to-tail arrangement. The QTAIM analysis of this supramolecular architecture corroborates the anion–π and lone pair···π interactions with the presence of ring critical points (red) connecting the

aromatic rings with the anion (perchlorate oxygen atom) and lone pair electron (malonate oxygen atom) of adjacent monomers (**Figure 1.30**).[154]

Self-assembly of coordination solids has emerged as a topic of growing interest in biological applications.[155] After the use of arene ruthenium compounds (Tocher *et al*.) as anticancer agents in 1992, transition metal complexes have gained significant interest in bio-chemistry.[156] Therrien *et al*. have reported a cationic hexanuclear metalloprism $[Ru_6(p\text{-xylene})_6(tpt)_2(dhbq)_3]^{6+}$ [where, dhbq = 2,5-Dihydroxy-1,4-benzoquinone; tpt = 2,4,6-tris(pyridin-4-yl)-1,3,5-triazine][157]; the role of this Ru-based coordination complex in anticancer activity was mainly achieved by drug delivery, where the internal cavities of Ru-based host involving appropriate guests show desirable anticancer activities (**Figure 1.31**).[157] This host assembly exhibits trigonal prism geometry, whose internal cavity is capable of encapsulating guest molecules such as $[(acac)_2M]$ (M = Pd, Pt; acac = acetylacetonato).[157] Recently, the research group of Stang and Chi reported a series of such assembly with various diruthenium molecular clips (acceptors) (**Figure 1.32**).[158] The compounds are able to induce *in vivo* cytotoxicity against SK-hep-1 (liver), HeLa (cervix), HCT-15(colon), A-549 (lung), and MDA-MB-231 (breast) cancer cell lines.[158]

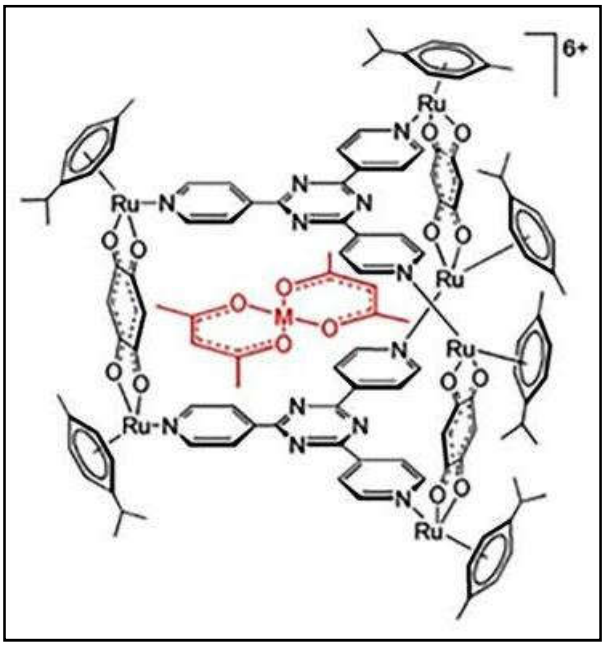

Figure 1.31 Ru-based assemblies in $[Ru_6(p\text{-xylene})_6(tpt)_2(dhbq)_3]^{6+}$ encaptulation of guest molecules of types $M(acac)_2$ [where, M = Pt and PD; acac = acetylacetonato].

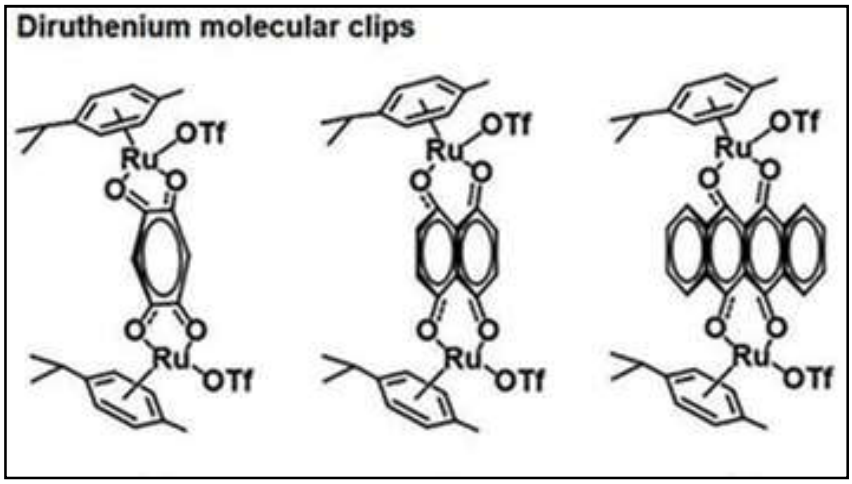

Figure 1.32 Diruthenium molecular clips that show *in vivo* cytotoxicity against various cancer cell lines.

Gogoi *et al*. have reported two Ni(II) coordination solids of pyrazole and acetato ligands, involving nitrate and chloride counter anions, *viz*. $[Ni(Hdmpz)_2(CH_3COO)(H_2O)_3]NO_3 \cdot 2H_2O$ and $[Ni(Hdmpz)_2(CH_3COO)(H_2O)_3]Cl$ [where, Hdmpz = 3,5-dimethylpyrazole and CH_3COO = acetate].[159] The supramolecular synthons (*vide supra*) of these two compounds are formed by $[Ni(Hdmpz)_2(H_2O)_3(CH_3COO)]^+$ cationic moiety with the respective counter anions (**Figure 1.33**). The compounds were reported to be effective in inducing *in vitro* cytotoxic potency against Dalton's Lymphoma malignant cancer cell lines.

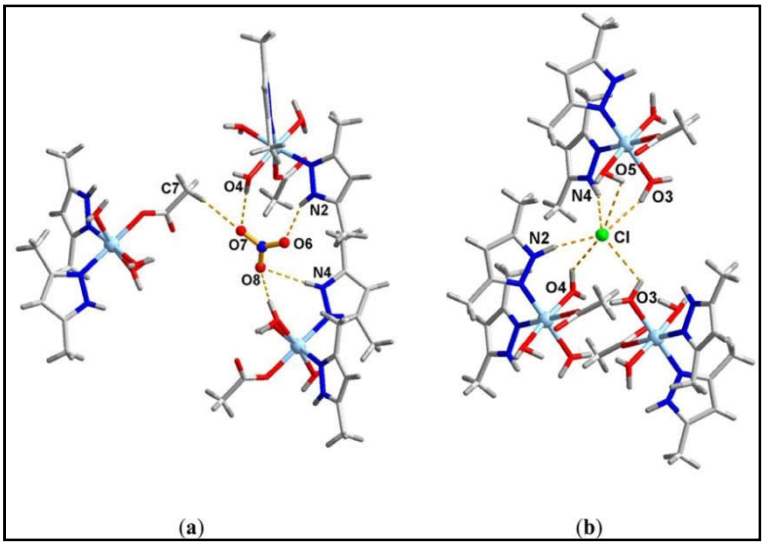

Figure 1.33 Supramolecular synthons formed by $[Ni(Hdmpz)_2(H_2O)_3(CH_3COO)]^+$ with (**a**) nitrate and (**b**) chloride anions.[159]

1.8 Anti-cancer Activities of Transition Metal Complexes

In the recent years, many transition metal complexes have been designed and synthesized to treat a wide variety of diseases.[160] Transition metal complexes have received remarkable emphasis in medicinal chemistry as diagnostic tools and anticancer agents.[161] The field of inorganic medicinal chemistry involves the administration (or removal) of a metal ion into (or from) a biological system for either diagnostic or therapeutic uses.[162] The property of transition metals to form positively charged ions in aqueous solution which can bind to negatively charged biological molecules make them potential candidates for the therapeutic uses.[163]

In recent years, various anticancer agents have been developed in the field of medicinal inorganic chemistry.[164] Although metals have been used in the treatment of various pathological disorders throughout human history, the full impact of metal-based compounds in the treatment of cancer has only been fully realized since the discovery of cisplatin. However, dose-dependent toxicity and resistance coupled with a narrow spectrum of activity limits its clinical use.[165] These limitations prompted the research for other platinum based compounds showing lower toxicity, higher selectivity and a broader spectrum of activities.[166] This search led to the generation of the complexes known as carboplatin and oxaliplatin.[167]

The ability of transition metal compounds to coordinate ligands in three dimensional configurations provides many advantages in the development of new medicinal compounds over conventional carbon-based compounds. This allows the synthesis of desired dimensionalities of functional groups that can be tailored to a target molecule.[168] In transition metals, the partially filled *d* orbitals offer interesting electronic properties, which can act as suitable probes for the design of anticancer agents.[169] Another important consideration in the design of coordination compounds is the oxidation state of a metal, since it allows participation in biological redox processes and plays an important role in bioavailability and optimal dose of the agent administered.[170] Furthermore, the metals can interact and coordinate to biological target molecules due to their ability to undergo ligand exchange reactions.[171]

MTT dye based cell viability and flourosense based apoptosis assays have been extensively exploited by various research groups to explore *in vitro* anticancer activities of coordination compounds.

1.8.1 MTT cell viability Assay

MTT cell viability assay is a widespread colourimetric estimation technique used to determine the percentage of viable/living cells present in a cell culture.[172] This assay can easily differentiate between live and dead cells on the basis of metabolic activity of the cells and hence it is superior to other cell viability techniques. This assay is based on the conversion of the MTT dye (*3-[4,5-dimethylthiazol-2-yl]-2,5 diphenyl tetrazolium bromide*) into purple colour formazan crystals by the living cells.[173] The healthy mitochondria of living cells can secret NADPH (*Nicotinamide Adenine Dinucleotide Phosphate Hydrogen*) dependent oxido-reductase enzyme. This enzyme can convert the MTT dye to water insoluble formazan crystals which is found to be soluble in organic solvents like DMSO. Hence, the mitochondrial activity of the living cells is reflected by the conversion of the tetrazolium MTT dye into formazan crystals. Thus, any increase or decrease in the number of viable cells can be detected by measuring formazan concentration reflected in optical density (OD) using a plate reader at 550 or 570 nm. MTT assay is the most widely used technique[174] to evaluate cytotoxic potential of clinical drugs, natural products and synthetic compounds for studying antiproliferative activity. Many research groups have recently explored this technique to investigate the cytotoxic potential of coordination compounds against various human cancer cell lines.[175] Castro-Ramirez and his research group have reported the DNA binding and cytotoxic potency of thirteen tinidazole (tnz) based coordination compounds of different geometries *viz*. $[M(tnz)_2(NO_3)_2]$ [where, M = Co, Cu, Ni, Zn]; $[M(tnz)_2Cl_2]$ [where, M = Co, Cu, Zn]; $[M(tnz)_2Br_2]$ [where, M = Co, Cu, Zn, Ni]; $[Cu(tnz)_2(\mu\text{-}Cl)Cl]_2$ and $[Cu(tnz)(\mu\text{-}AcO)_2]_2\cdot H2O$.[176]

1.8.2 Apoptosis Assay

The term apoptosis refers to a peculiar morphology of cell death which can be triggered physiologically, and it is regulated by the actions of specific gene products.[177] The general characteristics of apoptosis are distinct morphological features and biochemical mechanism. The various morphological changes taking place during apoptosis can be identified using light and electron microscope.[178] In the early apoptosis stage, cell shrinkage and chromatin condensation in the nucleus of the cell take place which are clearly visible under light microscope. Cell shrinkage is characterized by

smaller sizes of the cells, comparatively dense cytoplasm and more tightly packed organelles.[179] During the chromatin condensation phase, the electron-dense nuclear material characteristically aggregates peripherally under the nuclear membrane, although there can also be uniformly dense nuclei.[180] The classic method of apoptosis quantitation in laboratory is a simple microscopic observation, using blue light illumination and a pair of fluorescent dyes.[181] Acridine orange and ethidium bromide (AO/EB) dual staining method[182] is usually used to explore apoptosis inducing ability of chemotherapeutic drugs. AO is a vital fluorescent dye which can penetrate through cell membrane and is capable of staining nuclear DNA by intercalation between bases of viable/living cells and stained green, whereas EB can only stain apoptotic/dead cells and appears red or orange.[183] This colourimetric representation of viable and apoptotic cells suggests that AO/EB double staining method is a reliable and rapid assay to explore the apoptosis inducing ability of the drugs under investigation. Jadeja *et al*. have recently explored the *in vitro* apoptosis inducing ability of four pyrazolone based mixed ligand Cu(II) complexes, *viz*. [Cu(L1)(phen)NO_3], [Cu(L2)(bipy)NO_3], [Cu(L2)(phen)NO_3] and [Cu(L2)(bipy)NO_3] [where, phen = 1,10-phenanthroline; bipy = 2,2′-bipyridine; L1 = 3-methyl-5-oxo-1-phenyl-4,5-dihydro-1*H*-pyrazole-4-carbaldehyde; L2 = 4-(1-naphthoyl)-3-methyl-1-(*p*-tolyl)-1*H*-pyrazol-5(4*H*)-one] against human lung cancer cells.[184] Yan *et al*. have also explored the antiproliferative activity of a water soluble Zn(II) based metal-organic framework (MOF), *viz*. $[Zn_3(OH)_2(H_2tccp)_2(bipy)_2]\cdot 3H_2O\cdot 3DMF$ [where, H_4tccp = 2,3,5,6-tetrakis(4-carboxyphenyl)pyrazine, bipy = 4,4′-bipyridine] against human ovarian cancer cells.[185]

1.8.3 Cell Cycle and Cancer

In the human body, most of the cells are residing in "*out-of-cycle*" states instead of cycling. Only a small portion of them are actively cycling (proliferating), which are located mainly in the stem-transit amplifying compartments of self-renewing tissues, such as bone marrow and epithelia.[186] The process of replication of DNA and division of a cell consists of a series of coordinated events, called the "*cell division cycle*".

The cell cycle has four sequential phases (**Figure 1.34**). The most important phases among them are the S phase (when replication of DNA occurs) and M phase (when the cell divides into two cells). Two intermediate phases, referred as G1 and G2

separate these S and M phases. G1 takes place after mitosis when the cells are sensitive to both positive and negative cues from growth signaling networks. G2 is the gap after S phase when mitosis is about to take place.[187] G0 is another intermediate phase which describes a situation where cells in response to high cell density or mitogen deficiency are reversibly withdrawn from the cell division cycle.[188] The cyclin-dependent kinase (CDK) family of serine/threonine kinases and their regulatory partners (the cyclins) regulate the progression of the cell cycle.[189] G1 progression is driven by Cyclin D-CDK4, cyclin D-CDK6 and cyclin E-CDK2 through the restriction point committing the cell to complete the cycle.[190] Cyclin A-CDK2 initiates S phase, while cyclin B-CDK1 regulates progression through G2 and proceeds to mitosis.[191] Some sensor mechanisms monitor the progression through each cell cycle phase and the transition from one phase to the another. These are known as checkpoints, which maintain the correct order of events.[192] When the sensor mechanisms detect any incomplete cell cycle events (e.g. DNA damage), checkpoint pathways bring the signal to the effectors that cause the arrest of the cell cycle, until the problem is resolved.[193]

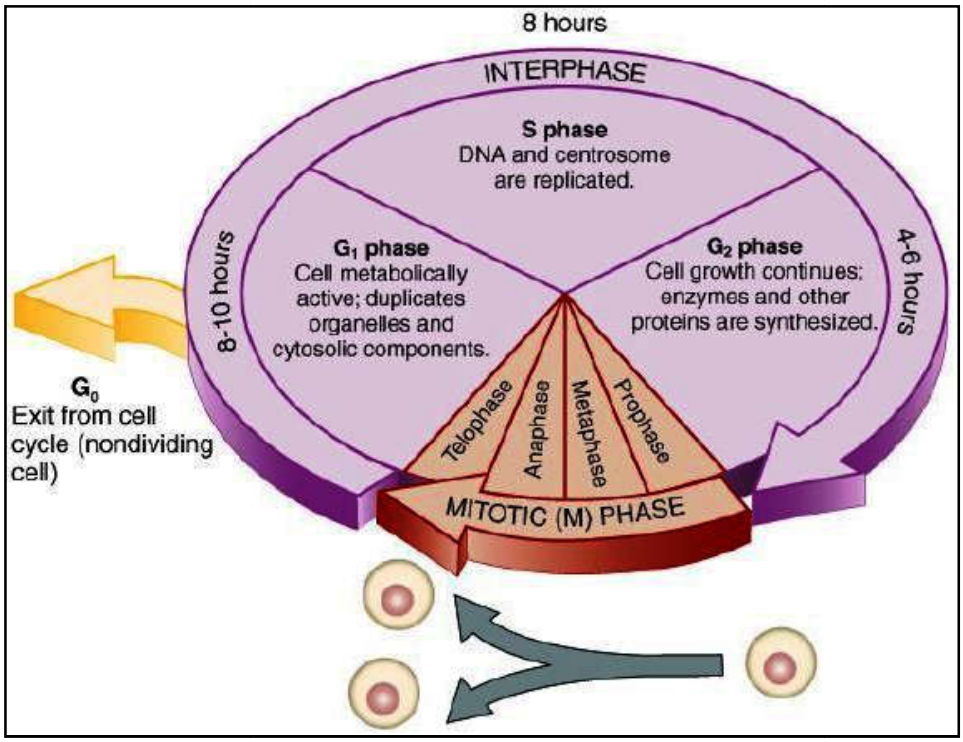

Figure 1.34 Schematic representation of the cell cycle.

The connection between cell cycle and cancer is that cell cycle controls the cell proliferation in human body, whereas cancer is a disease of inappropriate cell proliferation.[194] There are fundamental alterations in the genetic control of cell division that occurs during the cancer growth resulting in an uncontrolled cell proliferation. Basically, all the types of cancers allow the existence of too many cells resulting from the inappropriate cell proliferation. However, this excess in cell number is linked in a vicious cycle, which reduces the sensitivity to signals normally telling a cell to adhere, differentiate or die.[195] This combination of altered properties makes it difficult to identify the changes, which are primarily responsible for causing cancer disease.

1.8.4 Molecular Mechanism of Cisplatin

Cisplatin is a neutral square planar coordination complex. It induces its characteristic biological effects by reacting with DNA, which finally results in either repair of the damaged DNA and cell survival or activation of their reversible apoptotis. However, the neutral coordination complex cisplatin interacts with DNA only after it is activated through a series of spontaneous aquation reactions that involve the sequential replacement of the cis-chloro ligands with water molecules.[196] This hydrolyzed product is a potent electrophile, capable of reacting with any nucleophile, including the sulfhydryl groups on proteins and nitrogen donor atoms on nucleic acids.

The cytotoxicity of cisplatin is primarily due to its interaction with nucleophilic N7-sites of purine bases in DNA, whereby it forms DNA-protein and DNA-DNA inter-strand and intra-strand cross links.[197] This causes DNA damage in cancer cells, blocking the cell division and resulting in apoptotic cell death. However, strong evidence is there for intra-strand adducts as lesions largely responsible for the cytotoxic action.[198] This is corroborated by the fact that 1,2-intra-strand ApG and GpG [where, “p” is a phosphate linking the two bases; A = adenine; G = guanine] cross links are the major forms of DNA adducts.[199] Thus, it is well established that DNA is the critical target for cisplatin cytotoxicity. As illustrated in **Figure 1.35**, the cisplatin treatment of human cancers implicates several molecular mechanisms leading to apoptosis. Activation of a family of cysteine proteases, termed as caspases, is the key step in the initiation process of apoptosis.[200] p53, a short lived tumour protein caspase[201], plays a crucial role in the

apoptosis process. p53 is activated by ATR (*Ataxia Telangiectasia and Rad3-related protein; a vital sensor of reactive oxygen species*) on DNA damage signal. The activated p53 can transactivate genes involved in cell cycle progression, DNA repair and apoptosis. However, various transcription factors such as activation of mitogen-activated protein kinase (MAPK) cascade may lead to the drug resistance process.[202] The resistance of cisplatin by the cancer cells is a major complication in cancer chemotherapy which occurs when cancer cells do not respond to the anticancer drugs. Cisplatin resistance is reported to take place via several mechanisms[203]. As a consequence, to overcome the drug resistance in cancer chemotherapy, chemotherapeutic drugs alternative to cisplatin, *viz*. carboplatin[204] and oxaliplatin[205] have been developed. Various approaches have been made in recent times to explore new coordination complexes as cancer chemotherapeutic agents.[206]

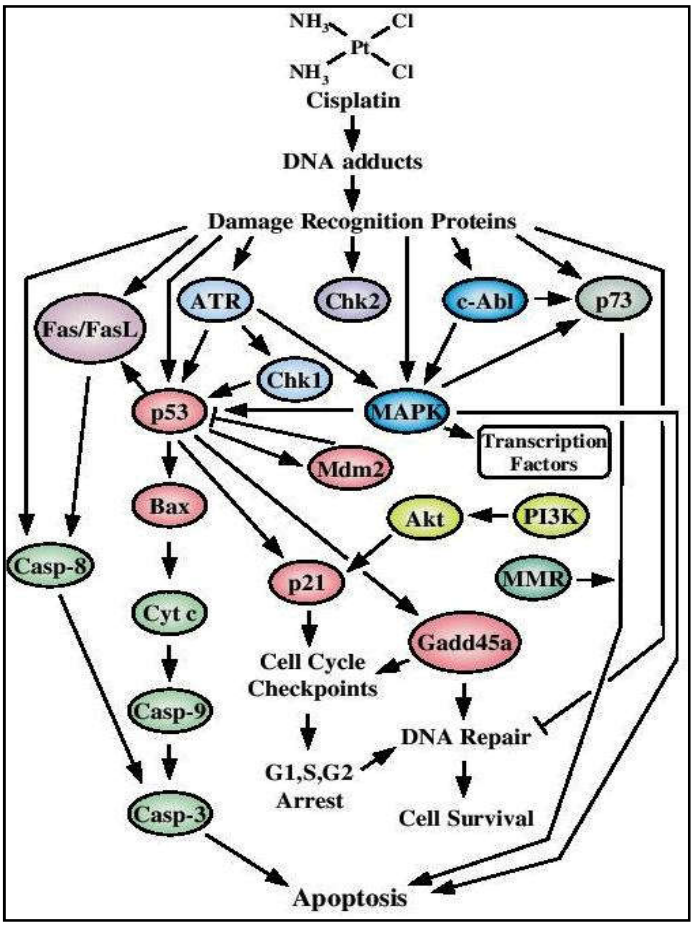

Figure 1.35 An overview of the pathways involved in mediating cisplatin-induced cellular effects.

1.9 Molecular Docking

Computational methods and screening strategies have remarkable impact in the development of new pharmaceutical drugs.[207] Most of the commercially available drugs are ligand-protein complexes, where the ligand enhances the activity of the protein to fight against the particular disease. Molecular docking is an important computational tool in the fields of medicinal biochemistry, computer-aided drug designing, computational structural biology and pharmacogenomics; because it can theoretically facilitate the probable ligand-receptor intereactions.[208] One important aspect is that docking provides certain information which is difficult to obtain through conventional experimental methods.

In simple words, docking tries to find the best "*fit*" between two molecules. Various types of docking procedures such as protein-ligand docking, protein-protein docking or nucleic acid-macromolecule docking play important roles in medicinal drug design. If interactions between two molecules take place, docking attempts to find out the best orientation in which the interactions are at their maximum with minimum binding energy.[209] In the case of a ligand-protein docking, the main objective is to predict the important binding pockets. This is done by searching high-dimensional spaces efficiently and thoroughly with the help of most effective docking softwares.

Molecular docking provides virtual screening of drug molecules with protein receptors (such as BCL family proteins) and widely used for lead identification in drug discovery programs. Molecular docking by Molegro Virtual Docker was performed for transitional metal complexes of Zn(II), Co(II), Cu(II), Fe(II), Ni(II)) involving cholic acid ligand against Aurora A Kinase receptor.[210] The result revealed that the complexes have potential action against Aurora A Kinase (*enzyme essential for cell proliferation*) inhibitor. The protein was retrieved from Protein Data Bank (PDB) (PDB ID: 2X6E).

Any molecule; be it a protein or a ligand; may undergo slight structural or conformational changes after it binds with another molecule. This causes slight difficulty in the analysis of the binding sites; which prompts the use of structure-based algorithms for this purpose.[211] Several molecular docking algorithms are now available which can fit or "*dock*" small molecules like ligands into pockets of macromolecules such as proteins or sometimes DNA, with different scoring and search algorithms[212], that can predict in an accurate and fast manner. For a given complex, these algorithms

in Molegro Virtual Docker (MVD) software determine all possible optimal conformations which are linked with a final MVD score. In addition, each of them calculates the energy of all the resulting conformations of each individual interaction.[213] The scoring functions (*which are mathematical functions*) assign a value based on the strength of the interactions between the two docked molecules. Each docked conformation is then scored for best fit.[214] Docking score only determines the best conformations for further research or for the purpose of developing a new drug.[215]

1.10 Pharmacophore Modelling

Pharmacophore modelling is a very successful and diverse subfield of computer-aided drug design (CADD) developed by Paul Ehrlich in the early 1900s.[216] At that time, it was understood that certain "*chemical groups*" or functions in a molecule were responsible for a particular biological effect, and that the molecules with similar effect had similar function in common. In 1960, Schueler coined the word pharmacophore in his book "*Chemobiodynamics and Drug Design*" as "*a molecular framework that carries the essential features responsible for a drug's (pharmacon) biological activity*".[217]

The International Union of Pure and Applied Chemistry (IUPAC), in 1997, defined pharmacophore as "*the ensemble of steric and electronic features that is necessary to ensure the optimal supramolecular interactions with a specific biological target and to trigger (or block) its biological response*".[218] A pharmacophore, thus, does not represent a real molecule or a set of chemical groups, rather it represents the largest common denominator of the molecular interaction features shared by a set of active molecules.

A pharmacophore model consists of a few characteristics organized in a specific 3D pattern.[219] Each feature is generally represented as a sphere (although variants exist), where the radius determines the tolerance on the deviation from the exact position (**Figure 1.36**).

Typical pharmacophore features include hydrophobic centroids, aromatic rings, hydrogen bond acceptors or donors, cations and anions.[220] These pharmacophore features may be located on the ligands themselves and responsible for their biological activities. It has been well established that pharmacophore features such as hydrophobic

centroids and aromatic rings play crucial roles in biological activities, as various drugs or complexes have been reported to bind with target biomolecules via aromatic π-stacking interactions.[221] As a consequence, coordination complexes involving ligands with extended aromatic rings may exhibit excellent biological activities due to their hydrophobic nature.[222]

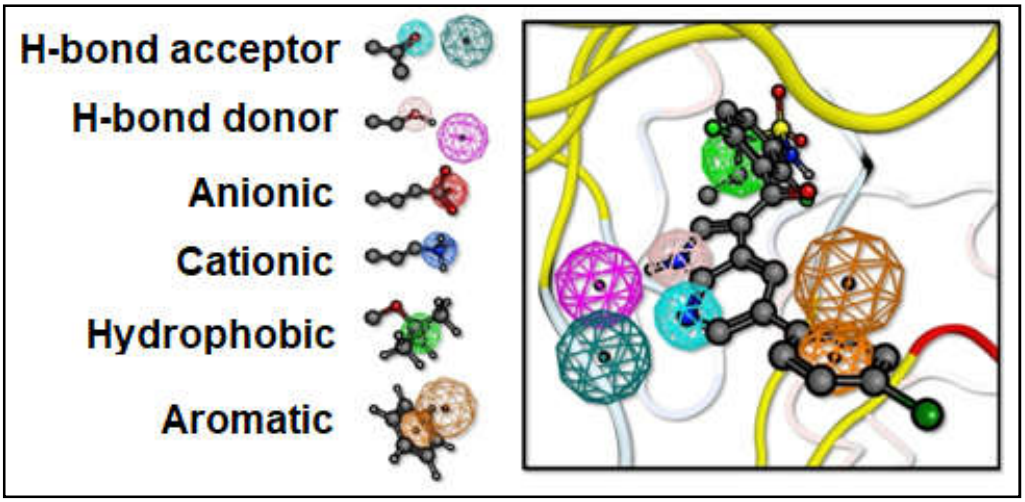

Figure 1.36 Model representing the pharmacophore features.

1.11 Aims and Objectives of the Present Thesis

In the present thesis work, we aim to design and synthesize supramolecular network architectures of transition metal coordination compounds having potentially important properties and applications. For this purpose, different first row transition metals including Mn, Co, Ni, Cu and Zn were used in combination with some multi-donor organic ligands (*2,5-pyridinedicarboxylate, 2,6-pyridinedicarboxylate etc.*) and N- donor ligands (*3-cyanopyridine, 4-cyanopyridine, pyridine etc.*).

After the synthesis of the coordination complexes, we aimed to characterize them by using various analytical, FT-IR and electronic spectroscopic techniques, thermogravimetric analyses, powder and single crystal X-ray diffraction techniques. We aim to grow suitable single crystals of representative compounds by the slow evaporation of the mother liquor to determine their crystal structures by single crystal X-ray diffraction. We also aim to explore the detailed X-ray structural analysis of the compounds to visualize the role of various non-covalent interactions in the stabilization

of supramolecular assemblies. Computational tools such as density functional theory (DFT), quantum theory of atoms in molecules (QTAIM), molecular electrostatic potential (MEP) surface analysis, non-covalent index (NCI) plot and symmetry-adapted perturbation theory (SAPT) shall be employed to study the various non-covalent interactions observed in the crystal structures of a few compounds.

We would also try to carry out antiproliferative activities of a few synthesized complexes against *Dalton's Lymphoma* (DL) malignant cancer cell line by using MTT cell viability and apoptosis assays. We shall also compare the cell viabilty results of the cancer cells with reference drug cisplatin. To further understand the possible mode of antiproliferative action of the compounds, we shall perform molecular docking study with some anti-apoptotic proteins. Our aim is also carryout pharmacophore study to identify the structure activity relationships (SAR) and the important pharmacophore features of the structures of the compounds responsible for the biological activities.

REFERENCES

1. (a) Nicolaou, K. C.; Hale, C. R. H.; Nilewski, C.; Ioannidou, H. A. *Chem. Soc. Rev*. **2012**, *41*, 5185.

(b) Gao, M.; Zhu, L.; Peh, C. K.; Ho, G. W. *Energ*. *Environ*. *Sci*. **2019**, *12*, 841.

2. (a) Vaxelaire, C.; Winter, P.; Christmann, M. *Angew. Chem. Int. Ed*. **2011**, *50*, 3605.

(b) Hajduk, P. J.; Galloway, W. J. R.; Spring, D. R. *Nature* **2011**, *470*, 42.

(c) O'Donnell, B. T.; Ives, C. J.; Mohiuddin, O. A.; Bunnell, B. A. *Bioeng. Biotechnol*. **2019**, *7*, 1.

3. (a) Rocca, J. D.; Liu, D.; Lin, W. *Acc. Chem. Res*. **2011**, *44*, 957.

(b) Cui, Q. H.; Zhao, Y. S.; Yao, J. *J. Mater. Chem*. **2012**, *22*, 4136.

(c) Zeng, Z.; Xu, Z.; Zhang, Z.; Gao, Z.; Luo, M.; Yin, Z.; Zhang, C.; Xu, J.; Huang, B.; Luo, F.; Du, Y.; Yan, C. *Chem. Soc. Rev*. **2020**, *49*, 1109.

4. (a) Xie, W.; Frisbie, C. D. *J. Phys. Chem*. **2011**, *115*, 14360.

(b) Lipomi, D. J.; Tee, B. C. K.; Vosguertichian, M.; Bao, Z. *Adv. Mater*. **2011**, *23*, 1771.

(c) Wu, W. *Sci. Technol. Adv. Mat*. **2019**, *20*, 187.

5. (a) Miyata, K.; Nishiyama, N.; Kataoka, K. *Chem. Soc. Rev*. **2012**, *41*, 2562.

(b) MacGillivray, L. R. *Angew. Chem. Int. Ed*. **2012**, *51*, 1110.

6. Pauling, L. *J. Am. Chem. Soc*. **1931**, *53*, 1367.

7. (a) Uhlenheuer, D. A.; Petkau, K.; Brunsveld, L. *Chem. Soc. Rev*. **2011**, *39*, 2817.

(b) Pijper, D.; Feringa, B. L. *Soft Matter* **2008**, *4*, 1349.

8. Lehn, J. M. *Supramolecular Chemistry Scope and Perspectives Molecules Supermolecules Molecular Devices*, In Nobel Lectures, Chemistry **1981-1990**, Frängsmyr, T. Ed. World Scientific Publishing Co. Singapore, **1992**.

9. Lehn, J. M. *Angew. Chem. Int. Ed*. **1990**, *29*, 1304.

10. (a) Christou, G.; Gatteschi, D.; Hendrickson, D. N.; Sessoli, R. *MRS Bull.* **2000**, *25*, 66.

(b) Gatteschi, D.; Sessoli, R. *Angew. Chem. Int. Ed.* **2003**, *42*, 268.

11. (a) Sessoli, R.; Gatteschi, D.; Caneschi, A.; Novak, M. A. *Nature* **1993**, *365*, 141.

(b) Wehner, M.; Rohr, M. I. S.; Bühler, M.; Stepanenko, S.; Wagner, W.; Würthne, F. *J. Am. Chem. Soc.* **2019**, *141*, 6092.

12. Brammer, L. *Dalton Trans*. **2003**, *16*, 3145.

13. Arunan, E.; Desiraju, G. R.; Klein, R. A.; Sadlej, J.; Scheiner, S.; Alkorta, I.; Clary, D. C.; Crabtree, R. H.; Dannenberg, J. P.; Hobza, P.; Kjaergaard, H. G.; Legon, A. C.; Mennucci, B.; Nesbitt; D. J. *Pure Appl. Chem*. **2011**, *83*, 1637.

14. (a) Grabowski, S. J. *Hydrogen Bonding-New Insights* **2006**.

(b) Afonin, A. V.; Vashchenko, A. V. *Int. J. Quantum Chem*. **2019**, *119*, 26001.

15. (a) Hunter, C. A. *Chem. Soc. Rev.* **1994**, *23*, 101.

(b) Vangala, V. R.; Nangia, A.; Lynch, V. M. *Chem. Commun.* **2002**, *12*, 1304.

16. (a) Desiraju, G. R. *Acc. Chem. Res.* **1991**, *24*, 290.

(b) Alkorta, I.; Elguero, J.; Frontera, A. *Crystals* **2020**, *10(3)*, 180.

17. Gerbier, P.; Domingo, N.; Gomez-Segura, J.; Ruiz-Molina, D.; Amabilino, D.; Tejada, J.; Williamson, B.; Veciana, J. *J. Mater. Chem.* **2004**, *14*, 2455.

18. (a) Jeffrey, G. A. *An Introduction to Hydrogen Bonding*, Oxford University Press ed., Oxford, **1997**.

(b) Desiraju, G. R. *Hydrogen Bonding*, in Encyclopedia of Supramolecular Chemistry **2004**.

19. Scatena, L. F.; Brown, M. G.; Richmond, G. L. *Science* **2001**, *292*, 908.

20. Alkorta, I.; Elguero, J.; Grabowski, S. J. *J. Phys. Chem. A* **2008**, *112*, 2721.

21. (a) Mandelgutfreund, Y.; Schueler, O.; Margalit, H. *J. Mol. Biol.* **1995**, *253*, 370.

(b) Dai, J.; Punchihewa, C.; Mistry, P.; Ooi, A.T.; Yang, D. *J. Biol. Chem*. **2004**, *279*, 46096.

(c) Wang, W.; Zhang, Y.; Liu, W. *Prog. Polym. Sci*. **2017**, *71*, 1.

(d) Anderson, A. J.; Culver, H. R.; Bryant, S. J.; Bowman, C. N. *Polym. Chem*. **2020**, *11*, 2959.

22. (a) Etter, M. C.; MacDonald, J. C.; Bernstein, J. *Acta Cryst*. **1990**, *B46*, 256.

(b) Etter, M. C. *Acc. Chem. Res*. **1990**, *23*, 120.

23. Aubin, S. M. J.; Sun, Z.; Eppley, H. J.; Rumberger, E. M.; Guzei, I. A.; Folting, K.; Gantzel, P. K.; Rheingold, A. L.; Christou, G.; Hendrickson, D. N. *Inorg. Chem.* **2001**, *40*, 2127.

24. (a) North, J. M.; *Ph.D. Thesis*, Florida State University, **2004**.

(b) Wilson, K. A.; Holland, D. J.; Wetmore, S. D. *RNA* **2016**, *22*, 696.

(c) Pineider, F.; Mannini, M.; Sangregorio, L.; Gorini, L.; Sessoli, R. *Inorg. Chim. Acta* **2008**, *361*, 3944.

25. Wheeler, S. E. *J. Am. Chem. Soc*. **2011**, *133*, 10262.

26. Hunter, C. A. *J. Am. Chem. Soc*. **1990**, *112*, 5525.

27. Sinnokrot, M. O.; Sherrill, C. D. *J. Phys.Chem. A* **2006**, *110*, 10656.

28. (a) Scott-Lokey, R.; Iverson, B. L. *Nature* **1995**, *375*, 303.

(b) Yan, T.; Yang, F.; Qi, S.; Fan, X.; Liu, S.; Ma, N.; Luo, Q.; Dong, Z.; Liu, J. *Chem. Commun*. **2019**, *55*, 2509.

29. (a) Li, H.; Zhang, X.; Zu, W. *J. Appl. Phys*. **2014**, *115*, 54510.

(b) Yu, W.; Wang, X. Y.; Li, J.; Li, Z. T.; Yan, Y. K.; Wang, W.; Pei, J. *Chem. Commun*. **2013**, *49*, 54.

30. Mas-Torrent, M.; Rovira, C. *Chem. Rev*. **2011**, *111*, 4833.

31. Bissell, R. A.; Córdova, E.; Kaifer, A. E.; Stoddart, J. F. *Nature* **1994**, *369*, 133.

32. (a) Liu, L.; Hao, J.; Shi, Y.; Qiu, J.; Hao, C. *RSC Adv*. **2015**, *5*, 3045.

(b) Shanmugaraju, S.; Mukherjee, P. S. *Chem.Commun*. **2015**, *51*, 16014.

33. Lipinski, C. A. *J. Pharmacol. Toxicol. Methods* **2000**, *44*, 235.

34. Sygula, A.; Fronczek, F. R.; Sygula, R.; Rabideau, P. W.; Olmstead, M. M. *J. Am. Chem. Soc.* **2007**, *129*, 3842.

35. (a) Perutz, M. F. *Q. Rev. Biophys*. **1989**, *22*, 139.

(b) Shinkai, S.; Ikeda, M.; Sugasaki, A.; Takeuchi, M. *Acc. Chem. Res*. **2001**, *34*, 494.

(c) Badjic, J. D.; Nelson, A.; Cantrill, S. J.; Turnbull, W. B.; Stoddart, J. F. *Acc. Chem. Res*. **2005**, *38*, 723.

(d) Mulder, A.; Huskens, J.; Reinhoudt, D. N. *Org. Biomol. Chem*. **2014**, *2*, 3409.

(e) Groizard, T.; Papior, N.; Guennic, B. L.; Robert, O. V.; Kepenekian, M. *J. Phys. Chem. Lett*. **2017**, *8*, 3415.

36. (a) Mammen, M.; Choi, S. K.; Whitesides, G. M. *Angew. Chem. Int. Ed*. **1998**, *37*, 2754.

(b) Ercolani, G. *J. Am. Chem. Soc*. **2003**, *125*, 16097.

(c) Hamacek, J.; Borkovec, M.; Piguet, C. *Dalton Trans*. **2006**, *12*, 1473.

37. Whitty, A. *Nat. Chem. Biol*. **2008**, *4*, 435.

38. Laos, A. J.; Dean, J. C.; Toa, Z. S. D.; Wilk, K. E.; Scholes, G. D.; Curmi, P. M. G.; Thordarson, P. *Angew. Chem. Int. Ed*. **2017**, *56*, 1.

39. Wroesky, H.; Andruh, M. *Coord. Chem. Rev*. **2003**, *236*, 91.

40. Sikorski, A.; Trzybiński, D. *J. Mol. Struct*. **2013**, *1049*, 90.

41. Wheeler, S.E.; Houk, K. N. *J. Am. Chem. Soc*. **2008**, *130*, 10854.

42. (a) Metrangolo, P.; Resnati, G. *Chem. Eur. J*. **2001**, *7*, 2511.

(b) Alkorta, I.; Blanco, F.; Deyà, P. M.; Elguero, J.; Estarellas, C.; Frontera, A. *D. Quiñonero Theor. Chem. Acc*. **2010**, *126*, 1.

(c) Galmés, B.; Martínez, D.; Infante-Carrió, M. F.; Franconetti, A.; Frontera, A.; *ChemPhysChem*. **2019**, *20*, 1135.

43. Vernon, R. M.; Chong, P. A.; Tsang, B.; Kim, T. H.; Bah, A.; Farber, P.; Lin, H.; Forman-Kay, J. D. *Struct. Biol. Mol. Biophys*. **2018**, *7*, 31486.

44. Bent, H. A. *Chem. Rev*. **1968**, *68*, 588.

45. (a) Echeverría, J. *Inorg. Chem*. **2018**, *57*, 5429.

(b) Islam, S. M. N.; Dutta, D.; Sharma, P.; Verma, A. K.; Frontera, A.; Bhattacharyya, M. K.; *Inorg. Chim. Acta* **2019**, *498*, 119108.

46. Wood, P. A.; Borwick, S. J.; Watkin, D. J.; Motherwell, W. D. S.; Allen, F. H. *Acta Crystallogr. Sect. B* **2008**, *64*, 393.

47. Desiraju, G. R.; Sharma, C. V. K. *Crystal engineering and molecular recognition-twin facets of supramolecular chemistry. In: Desiraju GR (ed) The crystal as a supramolecular entity:perspectives in supramolecular chemistry* **1996**.

48. (a) Desiraju, G. R.; Harlow, R. L. *J. Am. Chem. Soc.* **1989**, *111*, 6757.

(b) Merz, K. *Cryst. Growth Des*. **2006**, *6*, 1615.

49. Groom, C. R.; Bruno, I. J.; Lightfoot, M. P.; Ward, S. C. *Acta Cryst*. **2016**, *B72*, 171.

50. Dutta, D.; Islam, S. M. N.; Saha, U.; Frontera, A.; Bhattacharyya, M. K. *J. Mol. Struct*. **2019**, *1195*, 733.

51. (a) Politzer, P.; Murray, J. S.; Clark, T. *Phys. Chem. Chem. Phys*. **2010**, *12*, 7748.

(b) Clark, T.; Hennemann, M.; Murray, J. S.; Politzer, P. *J. Mol. Model*. **2007**, *13*, 291.

(c) Brinck, T.; Murray, J. S.; Politzer, P. *Int. J. Quantum Chem*. **1993**, *48*, 73.

(d) Politzer, P.; Lane, P.; Concha, M. C.; Ma, Y.; Murray, J. S. *J. Mol. Model*. **2007**, *13*, 305.

52. (a) Murray, J. S.; Lane, P.; Clark, T.; Politzer, P. *J. Mol. Model*. **2007**, *13*, 1033.

(b) Murray, J. S.; Lane, P.; Politzer, P. *Int. J. Quantum Chem*. **2007**, *107*, 2286.

(c) Politzer, P.; Murray, J. S. *Practical Aspects of Computational Chemistry*, Springer, Heidelberg, **2009**.

(d) Murray, J. S.; Riley, K. E.; Politzer, P.; Clark, T. *Aust. J. Chem*. **2010**, *63*, 1598.

53. Desiraju, G. R.; Ho, P. S.; Kloo, L.; Legon, A. C.; Marquardt, R.; Metrangolo, P.; Politzer, P.; Resnati, G.; Rissanen, K. *Pure Appl. Chem*. **2013**, *85*, 1711.

54. Bauza, A.; Mooibroek, T. J.; Frontera, A.; *ChemPhysChem*. **2015**, *16*, 2496.

55. Arunan, E.; Desiraju, G. R.; Klein, R. A.; Sadlej, J.; Scheiner, S.; Alkorta, I.; Clary, D. C.; Crabtree, R. H.; Dannenberg, J. J.; Hobza, P.; Kjaergaard, H. G.; Legon, A. C.; Mennucci, B.; Nesbitt, D. J. *Pure Appl. Chem*. **2011**, *83*,1637.

56. McGaughey, G. B.; Gagné, M.; Rappé, A. K. *J. Biol. Chem*. **1998**, *273*, 15458.

57. (a) Riley, K. E.; Murray, J. S.; Franfrlk, J.; Rezc, J.; Sol, R. J.; Concha, M. C.; Ramos, F. M.; Politzer, P. *J. Mol. Model*. **2011**, *17*, 3309.

(b) Stone, A. J. *J. Am. Chem. Soc*. **2013**, *135*, 7005.

58. Grabowski, S. J. *ChemPhysChem*. **2014**, *15*, 2985.

59. (a) Azofra, L. M.; Alkorta, I.; Scheiner, S. *Theor. Chem. Acc*. **2014**, *133*, 1586.

(b) Bauza, A.; Ramis, R.; Frontera, A.; *J. Phys. Chem. A* **2014**, *118*, 2827

60. A. Frontera, P. Gamez, M. Mascal, T. J. Mooibroek, J. Reedijk, *Angew. Chem. Int. Ed*. **2011**, *50*, 9564.

61. Berryman, O. B.; Bryantsev, V. S.; Stay, D. P.; Johnson, D. W.; Hay, B. P. *J. Am. Chem. Soc*., **2007**, *129*, 48.

62. Mascal, M.; Armstrong, A.; Bartberger, M. D. *J. Am. Chem. Soc*. **2002**, *124*, 6274.

63. (a) Caltagirone, C.; Gale, P. A. *Chem*. *Soc*. *Rev*. **2009**, *38*, 520.

(b) Estarellas, C.; Frontera, A.; Quiñonero, D.; Deyá, P. M. *Angew*. *Chem*. *Int*. *Ed*. **2011**, *123*, 435.

64. (a) Chifotides, H. T.; Dunbar, K. R. *Acc. Chem. Res.* **2013**, *46*, 894.

(b) Manna, P.; Seth, S. K.; Das, A.; Hemming, J.; Prendergast, R.; Helliwell, M.; Choudhury, S. R.; Frontera, A.; Mukhopadhyay, S. *Inorg. Chem*. **2012**, *51*, 3557.

(c) Rather, I. A.; Wagay, S. A.; Ali, R. *Coord. Chem. Rev*. **2020**, *415*, 213327.

65. Garau, C.; Frontera, A.; Quiñonero, D.; Ballester, P.; Costa, A.; Deyà, P. M. *J. Phys*. *Chem*. *A*, **2004**, *108*, 9423.

66. Quiñonero, D.; Deyà, P. M.; Carranza, M. P.; Rodríguez, A. M.; Jalón, F. A.; Manzano, B. R. *Dalton Trans*. **2010**, *39*, 794.

67. (a) Guralskiy, I. A.; Escudero, D.; Frontera, A.; Solntsev, P. V.; Rusanov, E. B.; Chernega, A. N.; Krautscheid, H.; Domasevitch, K. V. *Dalton Trans*. **2009**, *38*, 2856.

(b) Frontera, A. *Coord*. *Chem*. *Rev*. **2013**, *257*, 1716.

68. Schottel, B. L.; Chifotides, H. T.; Shatruk, M.; Chouai, A.; Perez, L. M.; Bacsa, J.; Dunbar, K. R. *J. Am. Chem. Soc*. **2006**, *128*, 5895

69. (a) Min, S. K.; Kim, W. Y.; Cho, Y.; Kim, K. S. *Nat. Nanotechnol*. **2011**, *6*, 162.

(b) Egli, M.; Gessner, R. V. *Proc*. *Natl*. *Acad*. *Sci*. **1995**, *92*, 180.

70. Mooibroek, T. J.; Gamez, P. *CrystEngComm.* **2012**, *14*, 1027.

71. Mooibroek, T. J.; Gamez, P.; Reedijk, J. *CrystEngComm*. **2008**, *10*, 1501.

72. Chapman, R. G.; Sherman, J. C. *Tetrahedron* **1997**, *47*, 15911.

73. Lehn, J. M. *Angew. Chem. Int. Ed. Engl.* **1988**, *27*, 89.

74. Fischer, E. *Ber. Dtsch. Chem. Ges.* **1894**, *27*, 2985.

75. (a) Belowich, M. E.; Valente, C.; Smaldone, R. A.; Friedman, D. C.; Thiel, J.; Cronin, L.; Stoddart, J. F. *J. Am. Chem. Soc.* **2012**, *134*, 5243.

(b) Zeng, F.; Zimmerman, S. C. *Chem. Rev.* **1997**, *97*, 1681.

(c) Gale, P. A. *Acc. Chem. Res.* **2006**, *39*, 465.

76. Sivakova, S.; Rowan, S. J. *Chem. Soc. Rev.* **2005**, *34*, 9.

77. (a) Philp, D.; Stoddart, J. F. *Angew. Chem. Int. Ed. Engl.* **1996**, *35*, 1154.

(b) Lindsey, J. S. *New J. Chem.* **1991**, *15*, 153.

(c) Whitesides, G. M.; Mathias, J. P.; Seto, C. T. *Science* **1991**, *254*, 1312.

78. Lehn, J. M.; Atwood, J. L.; Davies, J. E. D.; MacNicol, D. D.; Vbgtle, F. Pergamon: New York, **1996**.

79. Whitesides, G. M.; Mathias, J. P.; Seto, C. T. *Science* **1991**, *254*, 1312.

80. (a) Wu, G.; Chen, L.; Xu, L.; Zhao, X.; Yang, H. *Coord. Chem. Rev*. **2018**, *369*, 39.

(b) Kim, D. H.; Singh, N.; Oh, J.; Kim, E.; Jung, J.; Kim, H.; Chi, K. *Angew. Chem. Int. Ed*. **2018**, *57*, 5669.

81. (a) Han, F.; Yang, J.; Zhe, Y.; Chen, J.; Liu, J.; Li, R.; Jin, X.; Zhao, G. *Dalton Trans*. **2016**, *45*, 8862.

(b) Sasmal, H. S.; Halder, A.; Kunjattu, S. H.; Dey, K.; Nadol, A.; Ajithkumar, T. G.; Bedadur, P. R.; Banerjee, R. *J. Am. Chem. Soc*. **2019**, *141*, 20371.

82. Chapman, R. G.; Sherman, J. C. *Tetrahedron* **1997**, *47*, 15911.

83. Mack, J.; Stone, J.; Nyokong, T. J. *Porphyr. Phthalocya*. **2014**, *18*, 630.

84. Gonze, X. *Z. Krist. Cryst. Mater*. **2005**, *220*, 558.

85. Contreras-Garcia, J.; Johnson, E. R.; Keinan, S.; Chaudret, R.; Piquemal, J.; Beratan, D. N.; Yang, W. *J. Chem. Theo. Comput*. **2011**, *7*, 625.

86. AIMAll (Version 17.11.14), Keith, T. A. T.K Gristmill Software, Overland Park KS, USA, 2017.

87. Spartan'10, Wavefunction Inc. Irvine, CA.

88. Dreizler, R. M.; Gross, E. K. U. *Density Functional Theory-An Approach to the Quantum Many Body System*, **2012**.

89. Kolesov, G.; Kaxiras, E.; Manousakis, E. *Phys. Rev*. **2018**, *B98*, 195112.

90. (a) Hohenberg, P.; Kohn, W. *Phys. Rev.* **1964**, *136*, 864.

(b) Kohn, W.; Sham, L. J. *Phys. Rev.* **1981**, *B23*, 5048.

91. Li, G.; Rudshteyn, B.; Shee, J.; Weber, J. L.; Coskun, D.; Bochevarov, A. D.; Friesner, R. A. *J. Chem. Theory Comput*. **2020**, *16*, 2109.

92. (a) Segall, M. D.; Payne, M. C.; Ellis, S. W.; Tucker, G. T.; Boyes, R. N. *Phys. Rev*. **1998**, *E57*, 4618.

(b) Palafox, M. A.; Benial, A. M. F.; Rastogi, V. K. *Int. J. Mol. Sci*. **2019**, *20*, 3477.

93. (a) Shah, R.; Payne, M. C.; Lee, M. H.; Gale, J. D. *Science* **1996**, *271*, 1395.

(b) Kumar, G.; Tibbitts, L.; Newell, J.; Panthi, B.; Mukhopadhyay, A.; Rioux, R. M.; Pursell, C. J.; Janik, M.; Chandler, B. D. *Nat. Chem*. **2018**, *10*, 268.

94. Rutter, M. J.; Heine, V. *J. Phys. Condens. Matter* **1997**, *9*, 2009.

95. (a) Zeng, W. S.; Heine, V.; Jepsen, O. *J. Phys. Condens. Matter* **1997**, *9*, 3489.

(b) Erba, A.; Maul, J.; Ferrabone, M.; Carbonnière, P.; Rérat, M.; Dovesi, R. *J. Chem. Theory Comput*. **2019**, *15*, 3755.

96. Kirchhoffdag, F.; Gillandag, M. J.; Holenderdag, J. M.; Kresse, G.; Hafner, J. *J. Phys. Condens. Matter* **1996**, *47*, 2009

97. Aguilar, E. C.; Echeverría, G. A.; Piro, O. E.; Ulica, S. E.; Jios, J. L.; Tuttolomondo, M. E.; Pérez, H. *Mol. Phys*. **2018**, *116*, 399.

98. (a) Grimme, S.; Antony, J.; Schwabe, T.; Muck-Lichtenfeld, C. *Org. Biomol. Chem*. **2007**, *5*, 741.

(b) Murthy, P. K.; Smitha, M.; Mary, Y. S.; Armaković, S.; Armaković, S. J.; Rao, R. S.; Suchetan, P. A.; Giri, L.; Pavithran, R.; Alsenoy, C. V. *J. Mol. Struct*. **2017**, *1149*, 602.

99. (a) Mahlberg, D.; Sakong, S.; Forster-Tonigold, K.; Grob, A. *J. Chem. Theory Comput.* **2019**, *15*, 3250.

(b) Saha, U. S*ynthetic Approaches, Structural Investigations and Properties of Supramolecular Coordination Solids involving Phenanthroline Ligand,* Ph.D. Dissertation, Gauhati University, **2020**.

100. Peverati, R.; Baldridge, K. K. *J. Chem. Theory Comput.* **2008**, *4*, 2030.

101. (a) Burns, L. A.; Vázquez-Mayagoitia, Á.; Sumpter, B. G.; Sherrill, C. D. *J. Chem. Phys.* **2011**, *134*, 84107.

(b) Wang, L.; Gong, C.; Yuan, X.; Wei, G. *Nanomaterials* **2019**, *9*, 285.

102. Bader, R. F. W. *J. Phys*. *Chem*. *A* **2007**, *111*, 7966.

103. (a) Mohan, N.; Suresh, C. H.; Kumar, A.; Gadre, S. *Phys. Chem. Chem. Phys.* **2013**, *15*, 18401.

(b) Murray, J. S.; Paulsen, K.; Politzer, P. *Proc. Chem. Sci.* **1994**, *104*, 267.

104. (a) Politzer, P.; Murray, J. S.; Peralta-Inga, Z. *Int. J. Quantum Chem.* **2001**, *85*, 676.

(b) Politzer, P.; Murray, J. S.; Pollenaere, J. P.; Bultinck, P.; De-Winter, H.; Langenaeker, W. *Computational Medicinal Chemistry and Drug Discovery*, Dekker, New York, **2002**.

105. (a) Khan, I.; Panini, P.; Khan S. U.; Rana, U. A.; Andleeb, H.; Chopra, D.; Hameed, S.; Simpson, J. *Cryst. Growth Des*. **2016**, *16*, 1371.

(b) Varadwaj, A.; Marques, H. M.; Varadwaj, P. R. *Molecules* **2019**, *24*, 379.

106. Hunter, C. A. *Angew. Chem. Int. Ed*. **2004**, *43*, 5310.

107. Politzer, P.; Murray, J. S. *Theor. Chem. Acc*. **2002**, *108*, 134.

108. Tomasi, J.; Mennuci, B.; Cammy, M. *Molecular Electrostatic Potentials: Concepts and Applications*, ed. J. S. Murray and K. D. Sen, Elsevier, **1996**.

109. Contreras-Garcia, J.; Johnson, E. R.; Keinan, S.; Chaudret, R.; Piquemal, J. P.; Beratan, D. N.; Yang, W. *J. Chem. Theory Comput*. **2011**, *7*, 625.

110. Bader, R. F. W.; Esse´n, H. *J. Chem. Phys.* **1984**, *80*, 1943.

111. Kashyap, C.; Ullah, S. S.; Mazumder, L. J.; Guha, A. K. *Comput. Theor. Chem.* **2018**

112. (a) Bader, R. F. W. *Atoms in Molecules: A Quantum Theory*, Oxford University Press, Oxford, UK, **1990**.

(b) Bader, R. F. W. A. *Chem. Rev.* **1991**, *91*, 893.

113. Bader, R. F. W. *Acc. Chem. Res.* **1985**, *18*, 9.

114. Meyer, E. A.; Castellano, R. K.; Diederich, F. *Angew. Chem., Int. Ed. Engl*. **2003**, *42*, 1210.

115. Dunning, T. H. *J. Phys. Chem*. **2000**, *104*, 9062.

116. Stone, A. J. *The Theory of Intermolecular Forces*, Oxford University Press, Oxford, **2013**.

117. Jeziorski, B.; Moszynski, R.; Szalewicz, K. *Chem. Rev*. **1994**, *94*, 1887.

118. (a) Parker, T. M.; Burns, L. A.; Parrish, R. M.; Ryno, A. G.; Sherrill, C. D. *J. Chem. Phys*. **2014**, *140*, 94106.

(b) Szalewicz, K. *Comput. Mol. Sci*. **2012**, *2*, 254.

119. Szalewicz, K.; Jeziorski, B. *Molecular Interactions from van der Waals to strongly bound complexes,* edited by S. Scheiner, Wiley, New York, **1997**.

120. Braga, D. *Chem. Commun.* **2003**, *22*, 2751.

121. Desiraju, G. R. *Crystal Engineering: the Design of Organic Solids*, Elsevier, Amsterdam, **1989**.

122. Pacchioni, M.; Cornia, A.; Fabretti, A. C.; Zobbi, L.; Bonacchi, D.; Caneschi, A.; Chastanet, G.; Gatteschi, D.; Sessoli, R. *Chem. Commun.* **2004**, *21*, 2604.

123. (a) Aakeröy, C. B.; Seddon, K. R. *Chem. Soc. Rev.* **1993**, *22*, 397.

(b) Desiraju, G. R. *Angew. Chem. Int. Ed.* **1995**, *34*, 2311.

(c) Miyasaka, H.; Clerac, R.; Wernsdorfer, W.; Lecren, L.; Bonhomme, C.; Sugiura, K.; Yamashita, M. A. *Angew. Chem. Int. Ed.* **2004**, *43*, 2801.

124. Aubin, S. M. J.; Wemple, M. W.; Adams, D. M.; Tsai, H. L.; Christou, G.; Hendrickson, D. N. *J. Am. Chem. Soc.* **1996**, *118*, 7746.

125. (a) Schmidt, G. M. *J. Pure Appl. Chem.* **1971**, *27*, 647.

(b) Sarma, J. A. R. P.; Desiraju, G. R. *Acc. Chem. Res.* **1986**, *19*, 222.

(c) Etter, M. C. *J. Phys. Chem.* **1991**, *95*, 4601.

126. Desiraju, G. R. *Angew. Chem., Int. Ed.* **1995**, *34*, 2311.

127. Saha, S.; Desiraju, G. R. *Chem. Eur. J.* **2017**, *23*, 4936.

128. (a) Krishna, G. R.; Devarapalli, R.; Lal, G.; Reddy, C. M. *J. Am. Chem. Soc.* **2016**, *138*, 13561.

(b) Saha, S.; Desiraju, G. R. *Chem. Commun.* **2016**, *52*, 7676.

(c) Saha, S.; Desiraju, G. R. *J. Am. Chem. Soc.* **2017**, *139*, 1975.

129. (a) Hayashi, S. *Polym. J*. **2019**, *51*, 813.

(b) Worthy, A.; Grosjean, A.; Pfrunder, M. C.; Xu, Y.; Yan, C.; Edwards, G.; Clegg, J. K.; McMurtrie, J. C. *Nat. Chem*. **2018**, *10*, 65.

130. Liu, H.; Ye, K.; Zhang, Z.; Zhang, H.; *Angew. Chem. Int. Ed*. **2019**, *58*, 19081.

131. Kenny, E. P.; Jacko, A. C.; Powell, B. J. *Angew. Chem. Int. Ed*. **2019**, *58*, 15082.

132. Bhattacharya, B.; Michalchuk, A. A. L.; Silbernagl, D.; Rautenberg, M.; Schmid, T.; Feiler, T.; Reimann, K.; Ghalgaoui, A.; Sturm, H.; Paulus, B.; Emmerling, F. *Angew. Chem. Int. Ed*. **2020**, *59*, 5557.

133. MacGillivray, L. R.; Atwood, J. L. *J. Am. Chem. Soc.* **1997**, *119*, 6931

134. Huang, K. S.; Britton, D.; Etter, M. C.; Byrn, S. R. *J. Mater. Chem.* **1997**, *7*, 713.

135. Anthony, J. E.; Brooks, J. S.; Eaton, D. L.; Parkin, S. R. *J. Am. Chem. Soc.* **2001**, *123*, 9482.

136. Foxman, B. M.; Guarrera, D. J.; Taylor, L.D.; VanEngen, D.; Warner, J. C. *Mater. Res. Bull.* **1998**, *7*, 109.

137. (a) Almarsson, O.; Zaworotko, M. J. *Chem. Commun.* **2004**, *17*, 1889.

(b) Fleischman, S. G.; Kuduva, S. S.; Mcmahon, J. A.; Moulton, B.; Walsh, R. D. B.; Rodriguez-Hornedo, N.; Zaworotko, M. J. *Cryst. Growth Des.* **2003**, *3*, 909.

138. (a) MacGillivray, L. R.; Reid, J. L.; Ripmeester, J. A. *J. Am. Chem. Soc.* **2000**, *122*, 7817.

(b) Fowler, F. W.; Lauher, J. W. *J. Phys. Org. Chem.* **2000**, *13*, 850.

(c) Etter, M. C.; Frankenbach, G. M.; Bernstein, J. *Tetrahedron Lett.* **1989**, *30*, 3617.

139. Reddy, D. S.; Craig, D. C.; Desiraju, G. R. *J. Chem. Soc. Chem.* **1995**, *54*, 339.

140. (a) Usoltsev, A. N.; Adonin, S. A.; Novikov, A. S.; Samsonenko, D. G.; Sokolov, M. N.; Fedin, V. P. *CrystEngComm*. **2017**, *19*, 5934.

(b) Campillo-Alvarado, G.; Li, C.; Swenson, D. C.; MacGillivray, L. R. *Cryst. Growth Des*. **2019**, *19*, 2511.

141. Corcy, E. J. *Pure Appl. Chem.* **1967**, *14*, 19.

142. Desiraju, G. R. *Angew. Chem. Int. Ed. Engl.* **1995**, *31*, 2311.

143. Dutta, D.; Nath, H.; Frontera, A.; Bhattacharyya, M. *Inorg. Chim. Acta* **2019**, *487*, 354.

144. Lee, J.; Lee, L. M.; Arnott, Z.; Jenkins, H.; Britten, J. F.; Vargas-Baca, I. *New J. Chem*. **2018**, *42*, 10555.

145. Paulini, R.; Müller, K.; Diederich, F. *Angew. Chem. Int. Ed*. **2005**, *44*, 1788.

146. Woźniak, K.; He, H.; Klinowski, J.; Jones, W.; Grech, E. *J. Phys. Chem*. **1994**, *98*, 13755.

147. Steed, J. W.; Atwood, J. L. *Supramolecular Chemistry*, John Wiley & Sons, Hoboken, **2009**.

148. Albrecht, M. *Nat. Sci.* **2007**, *94*, 951.

149. Bilbeisi, R. A.; Olsen, J. C.; Charbonnière, L. J.; Trabolsi, A. *Inorg. Chim. Acta* **2014**, *417*, 79.

150. Voda, I.; Makhloufi, G.; Druta, V.; Lozana, V.; Shova, S.; Bourosh, P.; Kravtsov, V.; Janiak, C. *Inorg. Chim. Acta* **2018**, *482*, 526.

151. Mistri, S.; Zangrando, E.; Manna, S. C. *Inorg. Chim. Acta* **2013**, *405*, 331.

152. Manna, S. C.; Mistri, S.; Patra, A.; Mahish, M. K.; Saren, D.; Manne, R. K.; Santra, M. K.; Zangrando, E.; Puschmann, H. *Polyhedron* **2019**, *171*, 77.

153. (a) Heine, M.; Fink, L.; Schmidt, M. U. *CrystEngComm.* **2020**, 22, 2067.

(b) Heine, M.; Fink, L.; Schmidt, M. U. *CrystEngComm.* **2019**, *21*, 4305.

154. Robertazzi, A.; Krull, F.; Knapp, E. W.; Gamez, P. *CrystEngComm.* **2011**, *13*, 3293.

155. (a) Therrien, B. *Front. Chem*. **2018**, *6*, 602.

(b) Murray, B. S.; Dyson, P. J. *Curr. Opin. Chem. Biol*. **2020**, *56*, 28.

156. Zhang, X.; Liu, D, Lv F.; Yu, B.; Shen, Y.; Cong, H. *Colloids Surf. B* **2019**, *10*, 110373.

157. Therrien, B.; Süss-Fink, G.; Govindaswamy, P.; Renfrew, A. K.; Dyson, P. J. *Angew. Chem., Int. Ed.* **2008**, *47*, 3773.

158. Cook, T. R.; V. Vajpayee, V.; Lee, M. H.; Stang, P. J.; Chi, K. W. *Acc. Chem. Res.* **2013**, *46*, 2464.

159. Gogoi, A.; Dutta, D.; Verma, A.K.; Nath, H.; Frontera, A.; Guha, A. K.; Bhattacharyya, M. K. *Polyhedron* **2019**, *168*, 113.

160. Chen, D.; Milacic, V.; Frezza, M.; Dou, Q. P. *Curr. Pharm. Des.* **2009**, *15*, 777.

161. (a) Yan, Y. K.; Melchart, M.; Habtemariam, A.; Sadler, P. J. *Chem. Commun.* **2005**, 4764.

(b) Frezza, M.; Hindo, S.; Chen, D.; Davenport, A.; Schmitt, S.; Tomco, D.; Ping, D. *Curr. Pharm. Des*. **2010**, *16*, 1813.

162. Scott, L. E.; Orvig, C. *Chem. Rev.* **2009**, *109*, 4885.

163. (a) Yang, T.; Hussain, A.; Bai, S.; Khalil, I. A.; Harashim, H.; Ahsan, F. J. *Control. Release* **2006**, *115*, 289.

164. Zhao, G.; Lin, H. *Curr. Med. Chem. Anticancer Agents* **2005**, *5*, 137.

165. (a) Weiss, R. B.; Christian, M. C. *Drugs* **1993**, *46*, 360.

166. (a) Wong, E.; Giandomenico, C. M. *Chem. Rev.* **1999**, *99*, 2451.

(b) Ho, Y. P.; Au-Yeung, S. C.; To, K. K. *Med. Res. Rev.* **2003**, *23*, 633.

167. Rixe, O.; Ortuzar, W.; Alvarez, M.; Parker, R.; Reed, E.; Paull, K.; Fojo, T. *Biochem. Pharmacol*. **1996**, *52*, 1855.

168. Fricker, S. P. *Dalton Trans.* **2007**, *43*, 4903.

169. Hambley, T. W. *Dalton Trans.* **2007**, *43*, 4929.

170. (a) Orvig, C.; Abrams, M. J. *Chem. Rev.* **1999**, *99*, 2201.

(b) Thompson, K. H.; Orvig, C. *Sci.* **2003**, *300*, 936.

171. Fricker, S. P. *Dalton Trans.* **2007**, *43*, 4903.

172. Teixeira, R. R.; Barbosa, L. C.; Maltha, C. R. A.; Rocha, M. E.; Bezerra, D. P.; Costa-Lotuf, L. V.; Pessoa, C.; Moraes, M. O. *Molecules* **2007**, *12*, 1101.

173. Meerloo, J. V.; Kaspers, G. J. L.; Cloos, J. *Cancer Cell Culture* **2011**, *731*, 237.

174. Jamalian, A.; Miri, R.; Firuzi, O.; Amini, M.; Moosavi-Movahedi, A.; Shafieea, A. *J. Iran. Chem. Soc*. **2011**, *8*, 983.

175. (a) Jia, S.; Hao, X.; Wen, Y.; Zhang, Y. *J. Coord. Chem*. **2019**, *72*, 633.
(b) Aljamali, N. M.; Kadhim, A. J.; Mohammed, J. H.; Ghafil, R. A. A. *Int. J. Therm. Chem. Kinet*. **2019**, *5*, 23.
176. Castro-Ramírez, R.; Ortiz-Pastrana, N.; Caballero, A. B.; Zimmerman, M. T.; Stadelman, B. S.; Gaertner, A. A. E.; Brumaghim, J. L.; Korrodi-Gregório, L.; Pérez-Tomás, R.; Gamez, P.; Barba-Behrens, N. *Dalton Trans*. **2018**, *47*, 7551.
177. Reed, J. C. *Am. J. Clin. Pathol*. **2000**, *157*, 1415.
178. Kerr, J. F.; Wyllie, A. H.; Currie, A. R. *Br. J. Cancer* **1972**, *26*, 239.
179. Elmore, S. *Toxicol. Pathol*. **2007**, *35*, 495.
180. Osmani, S. A.; Engle, D. B.; Doonan, J. H.; Morris, N. R. *Cell* **1988**, *52*, 241.
181. Squier, M. K. T.; Cohen, J. J. *Mol. Biotechnol*. **2001**, *19*, 305.
182. Ciniglia, C.; Pinto, G.; Sansone, C.; Pollio, A. *Allelopathy J*. **2010**, *26*, 301.
183. Xu, X.; Gao, X.; Jin, L.; Bhadury, P. S.; Yuan, K.; Hu, D.; Song, B.; Yang, S. *Cell Div*. **2011**, *6*, 1.
184. Jadeja, R. N.; Vyas, K. M.; Upadhyay, K. K.; Devkar, R. V. *RSC Adv*. **2017**, *7*, 17107.
185. Yan, Z.; Li, X.; Fan, Q.; Bai, H.; Wu, S.; Zhang, Z.; Pan, L. *J. Mol. Struct*. **2020**, *1204*, 127477
186. Potten, C. S.; Loeffler M. *Development* **1990**, *110*, 1001.
187. Murray, A.; Hunt, T. *The Cell Cycle: An Introduction*. Oxford University Press: New York, **1993**.
188. Zetterberg, A.; Larsson, O. *Proc. Natl. Acad. Sci.* **1985**, *82*, 5365.
189. Malumbres, M.; Barbacid, M. *Cancer Cell* **2006**, *9*, 2.
190. Planas-Silva, M. D.; Weinberg, R. A. *Curr. Opin. Cell. Biol.* **1997**, *9*, 768.
191. Nigg, E. A. *Nat. Rev. Mol. Cell Biol.* **2001**, *2*, 21.
192. Hartwell, L. H.; Weinert, T. A. *Science* **1989**, *246*, 629.
193. (a) Bartek, J.; Lukas, C.; Lukas, J. *Nat. Rev. Mol. Cell. Biol.* **2004**, *5*, 792.
(b) Musacchio, A.; Salmon, E. D. *Nat. Rev. Mol. Cell. Biol.* **2007**, *8*, 379.
194. Wilhelm, S.M.; Carter, C.; Tang, L. *Cancer Res*. **2004**, *64*, 7099.
195. Huang, S.; Ingber, D. E. *Exp. Cell Res*. **2000**, *261*, 91.
196. Kelland, L. R. *Drugs* **2000**, *59*, 1.
197. Eastman, A. *Pharmacol. Ther*. **1987**, *34*, 155.

198. Pinto, A. L.; Lippard, S. J. *Biochim. Biophys. Acta* **1985**, *780*, 167.

199. Kelland, L. R. *Crit. Rev. Oncol. Hematol*. **1993**, *15*, 191.

200. Boice, A.; Bouchier-Hayes, L. *BBA-Mol. Cell Res*. **2020**, *1867*, 118688.

201. Blanco, J.; Lafuente, D.; Gómez, M.; García, T.; Domingo, J. L.; Sánchez, D. J. *Arch. Toxicol*. **2017**, *91*, 651.

202. Zlobin, A.; Bloodworth, J. C.; Osipo, C. *Predictive Biomarkers in Oncology* **2018**, 213.

203. Siddik, Z. H. *Oncogene* **2003**, *22*, 7265.

204. Wagstaff, A. J.; Ward, A.; Benfield, P.; Heel, R. C. *Drugs* **1989**, *37*, 162.

205. Lévi, F.; Metzger, G.; Massari, C.; Milano, G. *Clin. Pharmacokinet*. **2000**, *38*, 1.

206. (a) Usman, M.; Zaki, M.; Khan, R. A.; Alsalme, A.; Ahmad, M.; Tabassum, S.; *RSC Adv*. **2017**, *7*, 36056.

(b) Shahraki, S.; Majd, M. H.; Heydari, A. *J. Mol. Struct*. **2019**, *1177*, 536.

(c) Basu, U.; Roy, M.; Chakravarty, A. R. *Coord. Chem. Rev*. **2020**, *417*, 213339.

207. Durrant, J.; McCammon, J. A. *BMC Biology* **2011**, *9(1)*, 71.

208. Gulati, S.; Cheng, T. M. K.; Bates, P. A. *Semin. Cancer Biol.* **2013**, *23(4)*, 219.

209. Gold, A. K. *Cyber infrastructure, data, and libraries*, part 2: Libraries and the data challenge: Roles and actions for libraries. Office of the Dean (Library), 17, **2007**.

210. Beteringhe, A.; Racuciu, C.; Balan, C.; Stoican, E., Patron, L. *Adv. Mater. Res*. **2013**, *787,* 236.

211. Ghersi, D.; Sanchez, R. *J. Struct. Funct. Genom*. **2011** *12*, 109.

212. (a) Friesner, R. A.; Banks, J. L.; Murphy, R. B.; Halgren, T. A.; Klicic, J. J.; Mainz, D. T.; Repasky, M. P.; Knol, E. H.; Shelley, M.; Perry, J. K.; Shaw, D. E.; Francis, P.; Shenkin, P. S. *J. Med. Chem.* **2004**, *47*, 1739.

(b) McGann, M. R.; Almond, H. R.; Nicholls, A.; Grant, J. A.; Brown, F. K. *Biopolymers* **2003**, *68*, 76.

213. Sushma, B.; Suresh, C. V. *J. Applicable Chem*. **2012**, *1(2)*, 167.

214. Zsoldos, Z.; Reid, D.; Simon, A.; Sadjad, S. B.; Johnson, A. P. *J. Mol. Graphics Model.* **2007**, *26(1)*, 198.

215. Alonso, H.; Bliznyuk, A. A.; Gready, J. E. *Med. Res. Rev.* **2006**, *26(5)*, 531.

216. Ehrlich, P. *Ber. Dtsch. Chem. Ges*. **1909**, *42(1)*, 17.

217. Schueler, F. W. *Chemobiodynamics and Drug Design*, New York; McGraw-Hill,

1960.

218. Wermuth, C. G.; Ganellin, C. R.; Lindberg, P.; Mitscher, L. A. *Pure Appl. Chem*. **1998**, *70*, 1129.

219. (a) Geppert, T. D.; Lipsky, P. E. *Crit. Rev. Immunol*. **1989**, *9(4)*, 313.

(b) Kutlushina, A.; Khakimova, A.; Madzhidov, T.; Polishchuk, P. *Molecules* **2018**, *23*, 3094;

220. (a) Sheridan, R. P.; Rusinko, A.; Nilakantan, R.; Venkataraghavan, R. *Proc. Natl. Acad. Sci. A*. **1989**, *86(20)*, 8165.

(b) Schaller, D.; Sribar, D.; Noonan, T.; Deng, L.; Nguyen, T. N.; Pach, S.; Machalz, D.; Bermudez, M.; Wolber, G. *Comput. Mol. Sci*. **2020**, *10*, 1468.

221. (a) Sudhamani, C. N.; Naik, H. S. B.; Ravikumar, T. R.; Prabhakara, M. C. *Spectrochim. Acta* **2009**, *72*, 643.

(b) Vovusha, H.; Sanyal, S.; Sanyal, B. *J. Phys. Chem. Lett*. **2013**, *4*, 3710.

222. M. Selvaganapathy, N. Raman, *J. Chem. Biol. Ther*. **2016**, *1*, 1000108-1000124